Nigerian Journal of Theoretical and Environmental Physics (NJTEP)
ISSN Print: 3026-9601
ISSN Online: 1597-9849
DOI: https://doi.org/10.62292/njtep.v3i3.2025.85
Volume 3(3), September 2025

Investigation of Groundwater Potential Zones Using Integrated Geophysical Techniques at Apaken Area, Sagamu, Southwestern Nigeria

***[1]Obafemi O. Ademolu, [1]Saheed A. Ganiyu, [1]Oluwaseun T. Olurin, [1]Kehinde D. Ajayi, [2]Adedeji A. Adetoyinbo, [1]Aderemi A. Alabi and [3]Adedayo A. Badejo**

[1]Department of Physics, Federal University of Agriculture, Abeokuta, Ogun State, Nigeria
[2]Department of Physics University of Ibadan, Oyo State Nigeria.
[3]Department of Civil Engineering, Federal University of Agriculture, Abeokuta, Ogun State, Nigeria

*Corresponding author's email: adeoba1974@gmail.com

ABSTRACT

Groundwater potential zones in Apaken Sagamu, South Western Nigeria was investigated using electrical resistivity and the natural electric field combined approaches. Twelve VES stations and six 2D electrical resistivity tomography (ERT) profiles were probed utilizing Schlumberger and Wenner array modes. respectively. The VES and 2D ERT data were processed and inverted using partial curve matching/WINRESIST and RES2DINV softwares, respectively. Natural electric field (NEF) technique was also employed on the traverses using PQWT. Three to five geo-electric layers are revealed by the results of the interpretation of the VES data: the topsoil, which has resistivity values between 55.5 and 747.3 Ωm and thicknesses between 0.4 and 2.9 m; laterite soil layer, which has resistivity values between 225.6 and 8985.8 Ωm and thicknesses between 0.8 and 18.3 m; sandy clay layer, which has resistivity values between 504.3 and 5477.8 Ωm and thicknesses between 6.5 and 34.6 m; and the layer of ferruginous medium to coarse sand, which has resistivity values between 603 and 4422.8 Ωm. The overburden thickness ranges from 1.2 to 24.0 m. Ferruginous fine sand layer of the VES stations constitutes the main aquifers' zone. Based on reflection coefficient and overburden thickness values used to infer groundwater yield status, 50% of total VES points had moderate to high groundwater yield whereas the remaining 50% exhibit very low to low groundwater potential. According to longitudinal conductance values of the overburden units, two marked aquifer protecting capability zones were pinpointed: the poor (91.67%) and weak (8.33%). The identified moderate to high groundwater yield zones (VES stations 4, 6 and 11) with their associated moderate protective capability were located on the west and northwest sides of the study area, and thus suggested for drilling. The result of 2D resistivity and NEF concur at traverses 3 and 4 indicating good yield of groundwater zones.

Keywords:
Sedimentary terrain,
Groundwater prospective sections,
Dar Zarrouk parameters,
Aquifer protective capability,
Ferruginous.

INTRODUCTION

All living things depend on water for nourishment and sustenance, and water makes up 70% of the Earth's surface. Nigeria's total area is 937,768 square kilometers, of which 13,000 are (CIA, 2013). Surface water and groundwater are typically the sources of drinking water. Earth's surface water bodies, like lakes, rivers, and reservoirs, are sources of surface water. Water is a necessary element and not only essential for drinking, it also plays a variety of other roles and is necessary for all developmental activities.

The need for water is highly increasing. Urbanization, industrialization, and population increase have made water sustainability and use more complicated in the modern world (Desersa et al., 2008). For the survival of all living things, groundwater is the "god-granted" natural resource, and it is most valuable and widely distributed resource on Earth which receives yearly replenishment from the abundant precipitation, unlike certain other mineral resources. Significant shared resources for household, agricultural, and industrial uses are groundwater resources (Kadam et al., 2019). For

whatever reason, water is a component of every growth, whether directly or indirectly.

Groundwater is kept and slowly travels through aquifers, which are rock layers that have the capacity to absorb and contain water. Aquifers are composed of soil, sand, and rocks. Ultimately, groundwater will return to the surface and finish the hydrologic cycle by emptying into lakes, oceans, springs, or other natural water sources. Around 33% of the water made available for human use comes from groundwater, which is found in aquifers beneath the surface of the land. Geologic formations that store water beneath are known as underground aquifers, and they are the source of groundwater. A well is drilled into the subterranean water supply, and the well water is pumped to the surface to obtain groundwater (Muchingami *et al.,* 2021; Gaikwad *et al.,* 2021; Olatinsu *et al.,* 2021; Adabanija *et al.,* 2021; Ifeanyichukwu *et. al., 2023).* The porosity of the layer or strata of geology that produces an aquifer determines utility of the aquifer as a groundwater source. (Gaikwad. *et al.,* 2021; Shang *et al.,* 2021; Kahal *et al.,* 2021; Gobashy *et al.,* 2021; Joel *et al.,* 2020).

The demand for groundwater by the people of Africa Continent is alarming due to increase in population, urbanization, industrialization, climate change and continuous loss of surface water quality to pollutants (Soomro *et al*., 2019; Wu *et al*., 2020: Agyemang 2021). Inadequate supply of tap water by the government to the populace necessitates the reason why individuals and organizations embark on drilling of alternative groundwater sources such as shallow well and deep bore holes (Ganiyu *et al*., 2022). However, it must be noted that the existence and distribution of groundwater in a particular area are influenced by factors such as topography, climate conditions, underlying rock types, geological structures, land use activities and their interaction with the hydrological features (Perrone and Jasechko, 2017; Oladunjoye *et al*., 2019: Wu *et al*., 2020; Arunbose *et al*., 2021). Most plentiful water supply for human use is found in groundwater. It is also the least expensive and consistently the highest quality and quantity. The occurrence quality of groundwater in various sites is greatly influenced by the local geological features. Groundwater is the water that exists below the water level in saturated soils and geological formations, and its movement is influenced by gravity (Tijani, 2017). The presence of groundwater, also known as an aquifer, is determined by the geological composition, landforms, and precipitation patterns of a particular region. Rainfall ultimately controls the amount of groundwater recovered from wells in any given locality. Groundwater can be accessed by boreholes, wells, and contact springs in the basement complex terrain. It can also be found in the worn regolith, fissures, and cracks in the newly crystalline rocks. Groundwater is the most prevalent water source in rural communities in Nigeria and has proven to be the most dependable resource for supplying water to these locations (Akoji, 2019). To maximize exploitation, the exploration calls for special methods. The intended outcome will be achieved by applying 2D resistivity and magnetization techniques. In some areas of the southwest Basement Complex terrain of Nigeria, Bayewu *et al.,* 2017, carried out a study on the geophysical evaluation of groundwater potential. In southwest Nigeria's Awa-Ilaporu, close to Ago Iwoye, the study's focus was on groundwater potential. Mostly made up of granite gneiss, pegmatite, and banded gneiss, the region is situated in the southwest of Nigeria, within the Crystalline Basement Complex. Two geophysical techniques; vertical electrical sounding (VES) and very low-frequency electromagnetic (VLF-EM) were used in identifying locations with high groundwater potential. Salami and Ogbamikhumi (2017) carried out a geo-electrical examination to determine the groundwater potential of Ihievbe Ogben, Edo North, Nigeria. Vertical electrical sounding research was conducted using the Schlumberger array setup. The study of hydrogeological parameters showed that the thickness of the cracked and weathered basement, the basement relief, and the overburden thickness in the basement all had different resistivity values. Tajudeen *et. al.* (2019) using the electrical resistivity approach for groundwater potential, a geophysical information survey of difficult basement terrain was conducted. The purpose was to offer geological and geophysical data regarding the area's apparent resistivity, groundwater, and subsurface layer geoelectric characteristics. Using Win-Resist and Suffer 8, the site's data were processed, and the resulting information was examined and interpreted. The results reasonably indicated that the aquifer units were composed of a cracked and worn layer that has substantial groundwater potential and is safe to contaminate.

Alabi (2020) conducted a study on groundwater exploration in a normal basement complex terrain in Alakia, Ibadan, Oyo State, Southwestern Nigeria. Using reflection potential from reflection coefficient and overburden thickness above bedrock, the study aims to identify fractured zones and areas with groundwater potential. Eight profiles were subjected to geoelectric measurement utilizing the Schlumberger array arrangement and the Vertical Electrical Sounding (VES) method. After the data was examined, it became clear that the region has a high groundwater prospect and is well fractured. Olayanju (2011) assessed the groundwater spring source in Akure, Southwestern Nigeria, by combining offset Wenner resistivity and Very Low Frequency Electromagnetic (VLF-EM) techniques of geophysical survey. It was argued that for

a successful groundwater exploration process, employing an integrated hydrogeological survey strategy produces better results. The groundwater potential in Ilara-Mokin, Akure, Nigeria, was determined by Falade et al. (2019) by integrating Vertical Electrical Sounding (VES) and Very Low Frequency Electromagnetic (VLF-EM) electrical resistivity approaches. The spots that are comparatively conductive with depth were identified by VLF-EM profiling, which was conducted on eight traverses. Based on the findings of the VLF-EM survey, eighteen VES stations were subsequently positioned along the six traverses heading east-west, with a maximum electrode separation of 65 meters. Combination of VLF-EM and VES adjudge to be helpful in investigating groundwater potential and suggest that borehole logging be modified to better define the aquifer in order to achieve better integration outcomes.

Aquifer units were mapped and described by Oladele and Odubote (2017) in a typical complex transition zone of Ijebu Ode using Vertical Electrical Soundings (VES) and geophysical logs. The research area lies in the region between the Cretaceous layers and Precambrian basement rocks of the Dahomey Basin in Southwest Nigeria (Osinowo and Olayinka 2012). With a maximum current electrode spacing of 900 m, sixteen VES were obtained using the Schlumberger array method. Four geoelectric layers were identified by interpreting the VES data, with the worn layer located at a subterranean depth of 80 meters. It is the researchers' opinion that there is little chance of groundwater exploration in the studied area. Aquifer characterization and groundwater recharge pattern investigations were also carried out by Badmus and Olatinsu (2010) at the Federal College of Education, Osiele Abeokuta, southwest Nigeria, in a typical basement complex formation. Schlumberger array with a 200 m electrode spacing was used for thirty-four (34) Vertical Electrical Sounding (VES) surveys. Topsoil, sandy clay, clayey sand, sandstone, shale/clay, fractured basement, and fresh basement are the seven different geologic formations that were found throughout their investigation. Principal aquiferous unit in the research region was determined to be the worn and fractured basement. Using Schlumberger array for collection of Vertical Electrical Sounding (VES) data, Mosuro *et al*. (2011) conducted geoprospecting research on groundwater exploration at Kobape, via Abeokuta, Southwest Nigeria. Agagu (1985), claimed that the Abeokuta group is part of the sedimentary landscape of the Dahomey Basin, which includes the Kobape area. With a lithology that is typically sandy and very resistant, four to five geoelectric strata were identified. A borehole should be dug during the hottest part of the dry season in order to access the research area's possible 270-meter-deep aquiferous layer.

Alabi et al. (2021) used integrated geophysical approaches to study the groundwater potential in Moloko-Asipa, Ogun State, Nigeria. The study's objectives were to pinpoint aquifer zones and provide information on the underlying lithology of the Moloko-Asipa region in southwest Nigeria. Throughout the survey, 10 vertical electrical soundings (VES) and eight traverses studied using the Very Low Frequency Electromagnetic (VLF-EM) approach with a consistent interval of sampling of 5 m were conducted. To determine the resistivity contrast across the selected profiles, measurements from the VLF-EM survey were processed using Karous and Hjelt filtering. Using Schlumberger array for the collection of Vertical Electrical Sounding (VES) data, Mosuro *et al.* (2011) carried out geophysical studies in southwest Nigeria via Abeokuta for groundwater drilling at Kobape. According to Agagu (1985), the Abeokuta group is part of the sedimentary landscape of the Dahomey Basin, which includes the Kobape area. Four to five geoelectric layers were identified, with a lithology that is typically sandy and very resistive. Geophysical. Potential aquiferous layer of the study area was found 270 meters deep and suggested drilling a borehole during the hottest part of the dry season in the area.

Gaikwad et al. (2021) used the VES technique and its derived Dar-Zarrouk parameters to identify groundwater potential zones (GPZ) in complex bedrock geological landscape. According to their findings, the most valuable locations for GPZ are the VES points located in the center of the Karli River Basin. suggested drilling a borehole at the height of the dry season in the area. There is dearth of research study making use of geophysical techniques to explore groundwater resources in the study area, hence, the need for his present study.

The goal of the current study is to use integrated geophysical approaches to investigate groundwater potential zones in the Apaken area of Sagamu, Southwestern Nigeria.

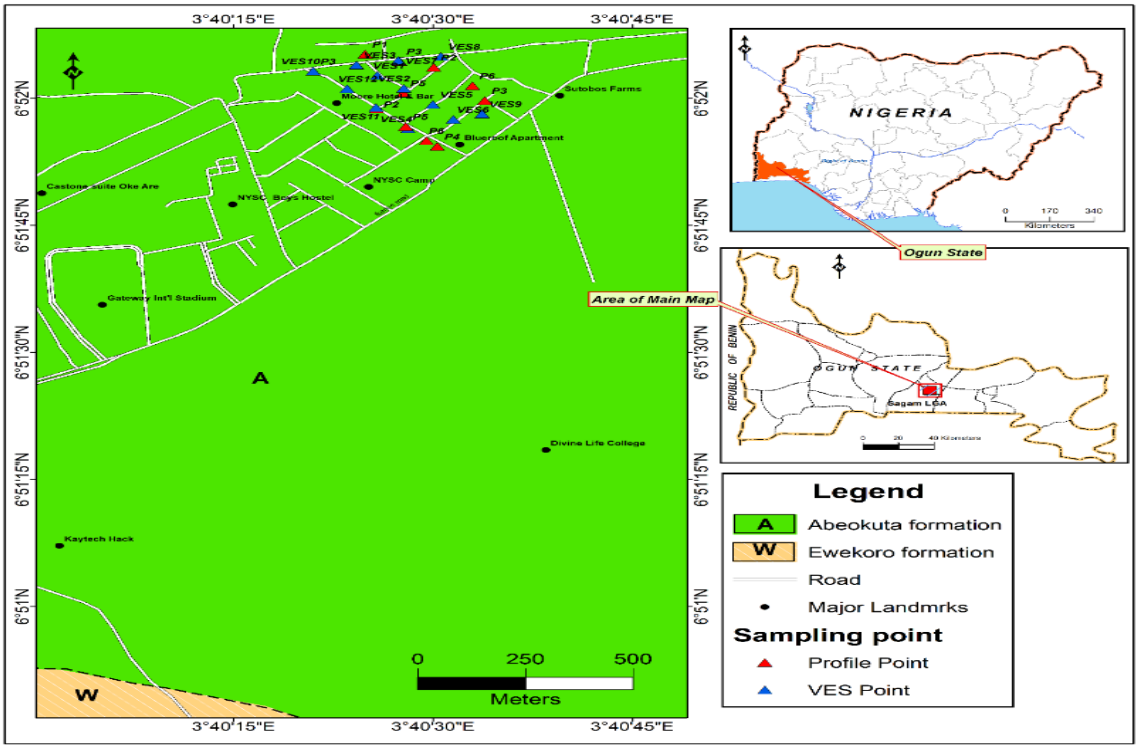

Figure 1: Map of the Study area showing Profile and VES Points

The study area lies between Latitudes 6 º 51' 56" N to 6 º 52' 5" North of the equator and between Longitudes 3 º 40' 20" E to 3º 40' 34" East of the Greenwich (Figure 1). It is largely located in Northwestern part of Sagamu Local Government Area. However, the study area slightly extends to a smaller part of Ikenne Local Government Area. This in other words means that it is located at the border boundary between Sagamu and Ikenne Local Government Area. Similarly, the study area is located within the National Youth Service Corps (NYSC) permanent Orientation Camp. It is equally bounded by Gateway International Stadium in Sagamu. It is therefore bunded in the north by Sagamu – Benin Expressway, and in the South by Ikenne road from Sagamu.The study area is characterized by gently undulating topography with average elevation of 260 m above sea level within the tropical humid region (Oyeyemi *et al*.2015). The vegetation of this area is mainly of the Rain forests type which is also found in areas like Ijebu lgbo, Odogbolu, and ljebu Ode in the eastern parts of Ogun State. Climate and relief have a major impact on the vegetation in the studied region. Due to the town's business and residential activity, there is currently little vegetation cover. Geology of this location is a sedimentary environment within Abeokuta formation extending to the South Eastern part of Ogun State and within the Eastern Dahomey basin (Oyeyemi *et al.* 2015).

MATERIALS AND METHODS

Vertical Electrical Sounding (VES)

Electrode separation (AB) in VES is widened from a stationary center. The deeper the stream penetrates the subsurface, the larger the gap (Reynolds, 1997).

Schlumberger array is used to suggest a current electrode spread (AB) of 1 to 200 meters. The ground potential difference created by the current flowing through points A and B is whose voltage is dictated by potential electrodes located at M and N (Wightman, 2003). Figure 4 shows sampling points in the study region.

Twelve (12) VES were acquired along six (6) traverses utilizing the Schlumberger electrode array setup depicted in Figure 6. Sampling places are indicated on the Sagamu study area location map. Two VES were conducted on each traverse line. The VES method Was employed by preserving the same relative distance between the current and potential electrodes, and the entire spread gradually grew along a profile. At the same center location, successive apparent resistivity values were calculated as the electrode spacing increased. The idea behind doing an electrical sounding, regardless of the electrode array that is employed, is that the deeper the investigation, the further the potential electrode is from the current source. Apparent resistivity was thus calculated:

$$\text{Apparent Resistivity } \rho = \pi R\left(\frac{L^2 - l^2}{2l}\right) \qquad (1)$$

Where R is Resistance in Ohm
ρ is the apparent resistivity
L is the distance between the current electrodes
l is the distance between the potential electrodes

Constant Separation Traversing (CST)

To identify the subsurface groundwater potential zones, a 2-D resistivity survey and associated interpretation model were used. The 2-D resistivity survey was conducted along the six (6) profiles using the Wenner electrode array configuration, Figure 8 (a to f). Measurements were made at sequences of electrodes interval of 10, 20 30, 40 and 50 m respectively. In using Wenner array configuration, the four electrodes were planted into the ground, moved along each profile at a constant electrode spacing (a) and successive readings were taken. The electrode spacing was varied for deeper imaging to obtain resistivity corresponding values for a = 10 m, 20 m, 30 m, 40 m, and 50 m for all the six (6) CST lines. Figure 6 shows data acquisition map generated for the survey site.

The inversion approach of the obtained data

The 2D computer software (RES2DINV) was used to invert the apparent resistivity measurement that was received from the 2D resistivity survey (Loke and Barker, 1996).

The inversion strategy involves using the 2D inversion procedure, a Gauss-Newton least square technique predicated on the subsurface 2D finite difference model (Sasaki, 1994).

Electromagnetic Method (PQWT – Groundwater Detector)

Among the new geophysical instruments is Portable Quantum Well Thermal (PQWT, Figure 7). This geophysical prospecting device is automatic and measures the earth's electromagnetic field in connection to lithological bodies. In the data input step, the potential electrodes convert the ambient field into a high-impedance electrical signal. The special built-in computational algorithms in PQWT improve data processing, and by converting analog to digital sampling, a frequency curve graph with a profile map is produced automatically (Kearey, 2012).

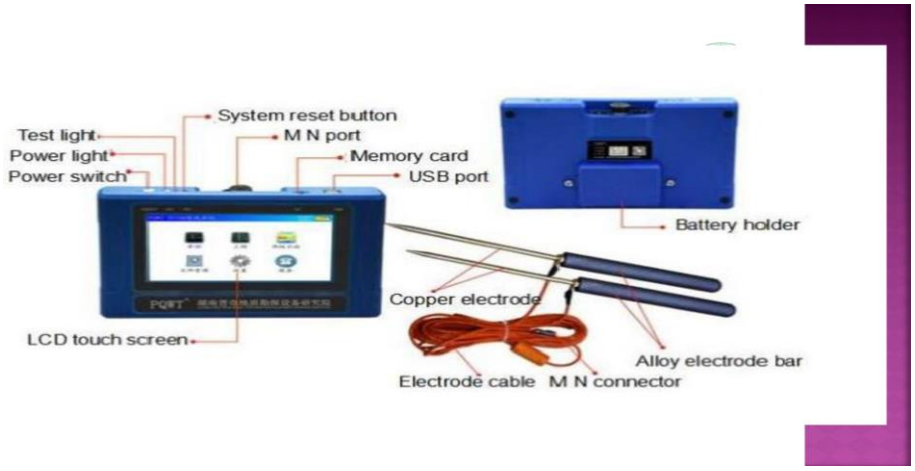

Figure 2: PQWT Equipment and Accessories

PQWT is a non invassive geophysical technique used for groundwater exploration. Data were obtained through the measurement of conductivity of the subsurface of the study area by employing the copper electrodes to inject a little electrical current into the ground at values of a = 10 m, 20 m, 30 m, 40 m, and 50 m, respectively. at regular spacing intervals of 10, 20, 30, 40 and 50 meters respectively along the six (6) profiles .

RESULTS AND DISCUSSION

The VES data from the Schlumberger array were shown on log-log graphs, with the values of half electrode separation (AB/2) and apparent resistivity (ρ) on the abscissa and ordinate, respectively. To determine the stacked apparent resistivities and thickness, the resulting curves were quantitatively analyzed using the partial curve matching approach and visual inspection. Figures 10 through 21 display the interpretation of the layer model and typical sounding curves from the site. These curves, which have three to five geo-electric layer combinations, are the A ($\rho1<\rho2<\rho3$), AK ($\rho1<\rho2<\rho3>\rho4$), KH ($\rho1<\rho2>\rho3<\rho4$), AKH ($\rho1<\rho2<\rho3>\rho4<\rho5$), and KHK ($\rho1<\rho2>\rho3<\rho4>\rho5$). The KH-curve types make up the majority, 58.3%, followed by the A-curve types (16.67%), and the remaining types of the AK, AKH, and KHK curves (8.33%). Figures 3 (a – l) display the VES curves produced from iterated VES data at the study location.

(a)

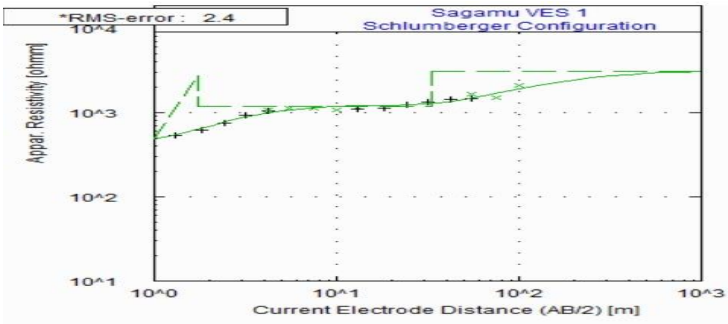

No	Res	Thick	Depth
1	427.1	1.0	1.0
2	2751.4	0.8	1.7
3	1186.7	31.3	33.0
4	3111.9	-.-	-.-

* RMS on smoothed data

(b)

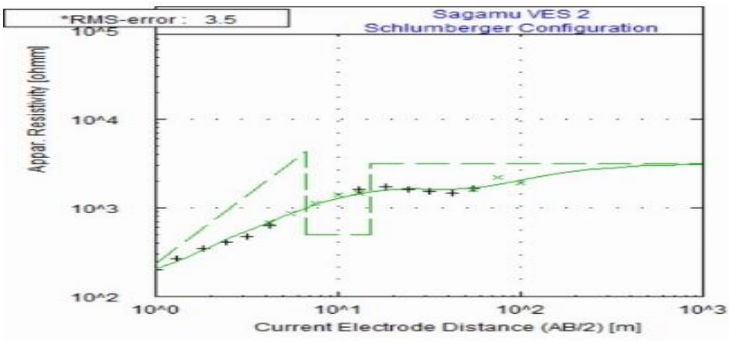

No	Res	Thick	Depth
1	134.6	0.7	0.7
2	4297.8	5.9	6.6
3	504.3	8.5	15.1
4	3127.4	-.-	-.-

* RMS on smoothed data

(c)

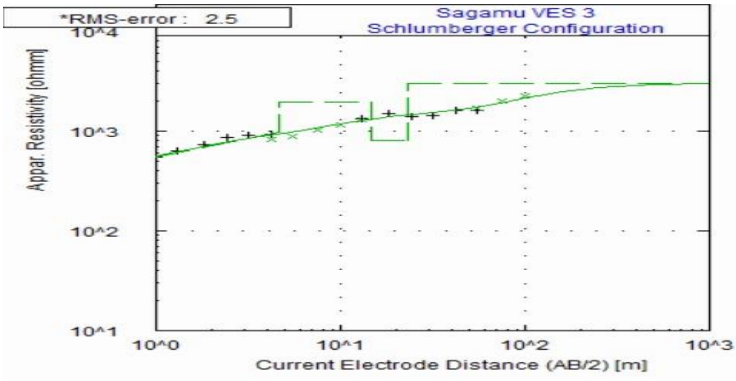

No	Res	Thick	Depth
1	409.3	0.5	0.5
2	985.8	4.2	4.7
3	1978.7	9.9	14.6
4	815.1	8.5	23.1
5	3047.0	-.-	-.-

* RMS on smoothed data

(d)

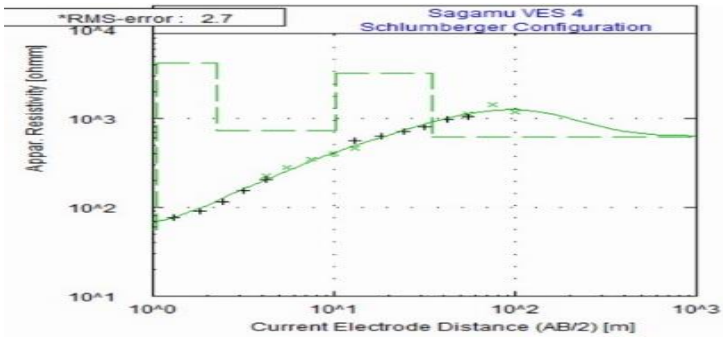

No	Res	Thick	Depth
1	56.8	1.1	1.1
2	4261.2	1.2	2.2
3	737.9	7.9	10.1
4	3244.9	24.4	34.6
5	625.9	-.-	-.-

* RMS on smoothed data

(e)

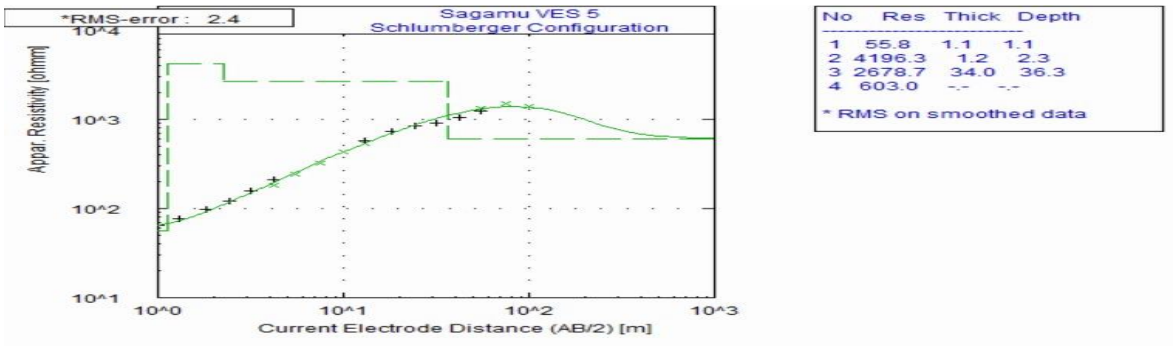
*RMS-error : 2.4
Sagamu VES 5
Schlumberger Configuration
Appar. Resistivity (ohmm)
10^4
10^3
10^2
10^1
10^0
10^1
10^2
10^3
Current Electrode Distance (AB/2) [m]
No Res Thick Depth
1 55.8 1.1 1.1
2 4196.3 1.2 2.3
3 2678.7 34.0 36.3
4 603.0 -.- -.-
* RMS on smoothed data

(f)

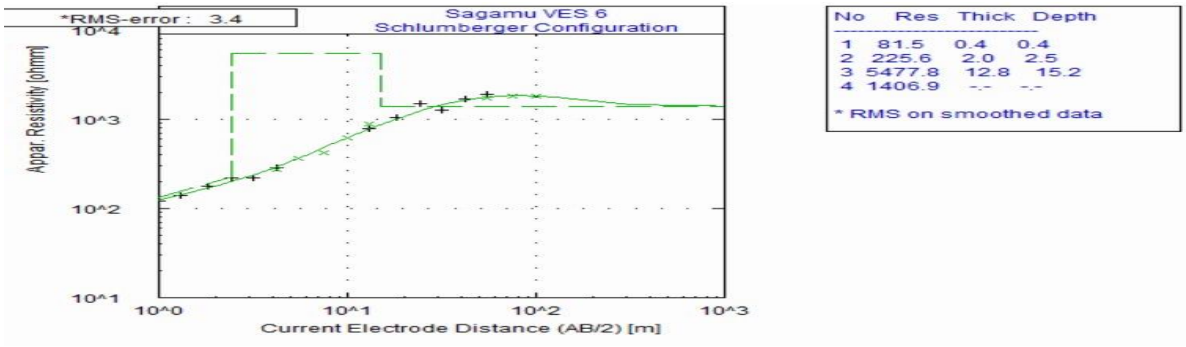
*RMS-error : 3.4
Sagamu VES 6
Schlumberger Configuration
Appar. Resistivity (ohmm)
10^4
10^3
10^2
10^1
10^0
10^1
10^2
10^3
Current Electrode Distance (AB/2) [m]
No Res Thick Depth
1 81.5 0.4 0.4
2 225.6 2.0 2.5
3 5477.8 12.8 15.2
4 1406.9 -.- -.-
* RMS on smoothed data

(g)

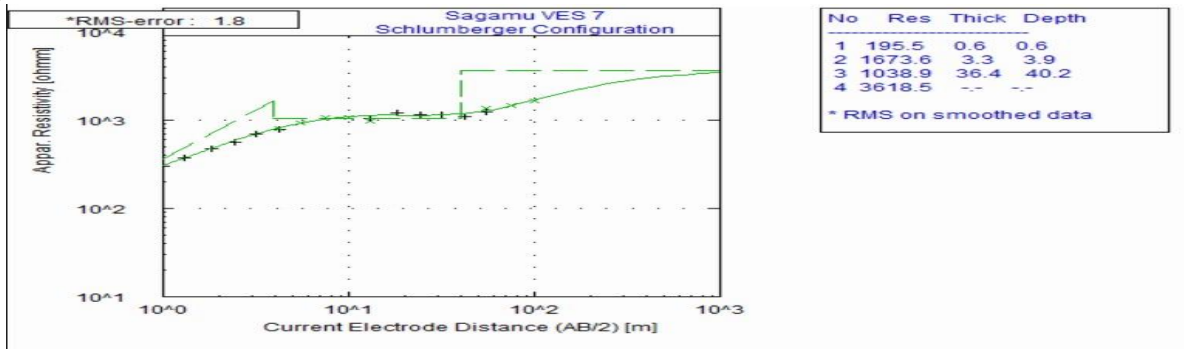
*RMS-error : 1.8
Sagamu VES 7
Schlumberger Configuration
Appar. Resistivity (ohmm)
10^4
10^3
10^2
10^1
10^0
10^1
10^2
10^3
Current Electrode Distance (AB/2) [m]
No Res Thick Depth
1 195.5 0.6 0.6
2 1673.6 3.3 3.9
3 1038.9 36.4 40.2
4 3618.5 -.- -.-
* RMS on smoothed data

(h)

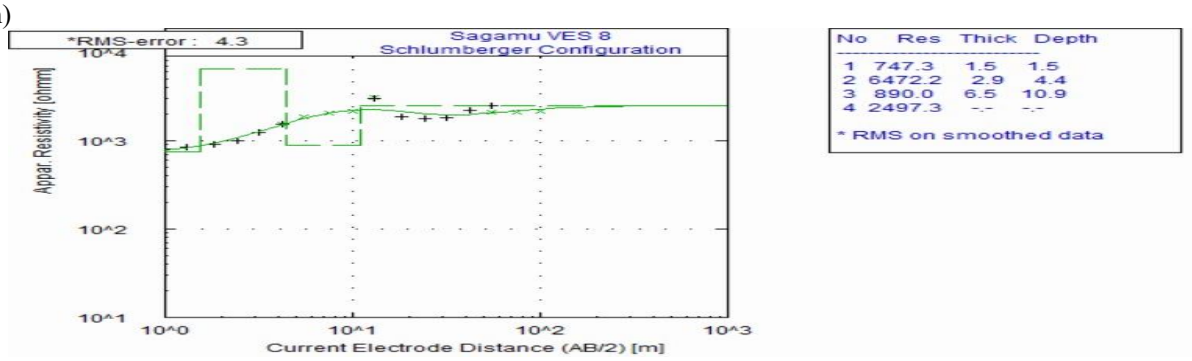
*RMS-error : 4.3
Sagamu VES 8
Schlumberger Configuration
Appar. Resistivity (ohmm)
10^4
10^3
10^2
10^1
10^0
10^1
10^2
10^3
Current Electrode Distance (AB/2) [m]
No Res Thick Depth
1 747.3 1.5 1.5
2 6472.2 2.9 4.4
3 890.0 6.5 10.9
4 2497.3 -.- -.-
* RMS on smoothed data

(i)

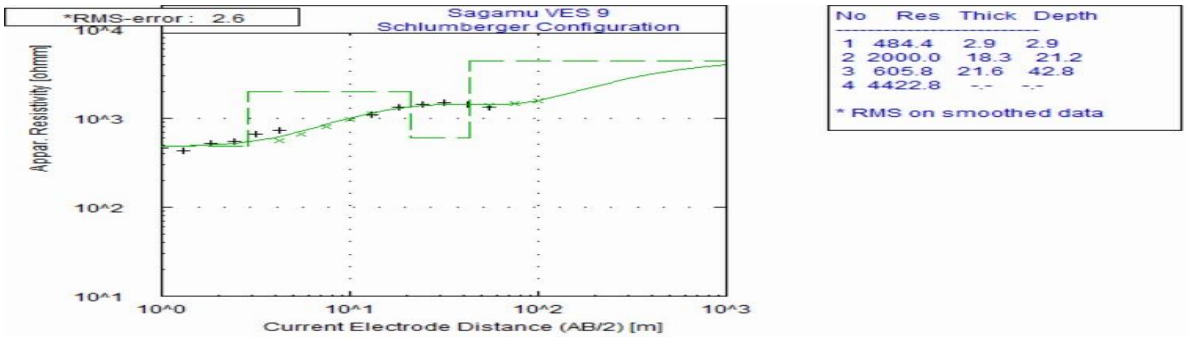

(j)

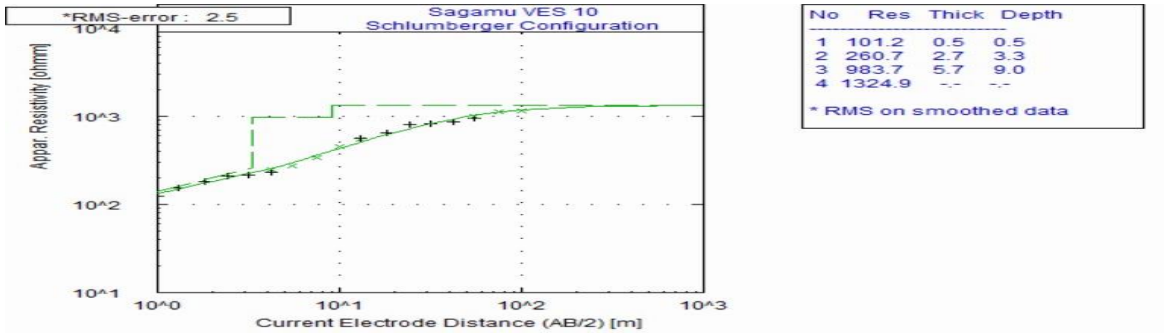

(k)

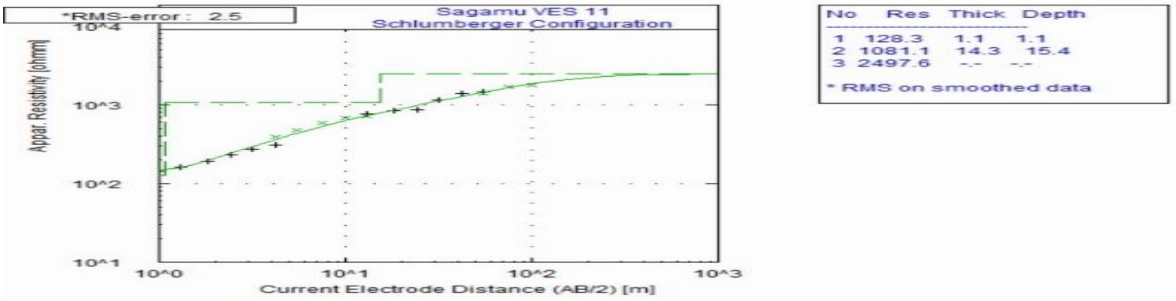

(*l*)

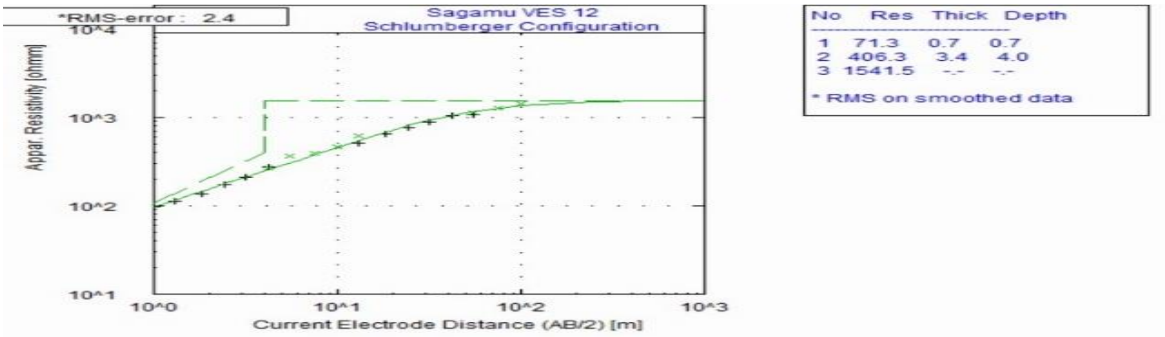

Figure 3 (*a* – *l*): Layer Model Interpretations for VES 1 to VES 12

Table 1 indicated a maximum of five geo-electric and geologic subsurface strata comprising resistivity values of 55.5 to 747.3 Ωm and thicknesses ranging from 0.4 to 2.9 m for the topsoil; resistivity values of 225.6 to 8985.8 Ωm for the laterite soil layer and thickness varying from (0.8 to 18.3) m; sandy clay layer with resistivity values between (504.3 to 5477.8) Ωm and the layer of ferruginous medium to coarse sand at the bottom line has an infinite thickness with resistivity values ranging from 603 to 4422.8% m. Its thickness varies from 6.5 to 34.6 m. The thickness of the overburden ranges from 1.2 to 24.0 meters. The primary aquifer zone is made up of the ferruginous fine sand layer found in the VES stations.

Table 1: Summary of the Geo-electric parameters for VES points in the study area

VES	Layer	Apparent Resistivity (ρ)	Thickness (m)	Depth (m)	Inferred Lithology	Curve Type
1	1	427	1.0	1.0	Topsoil	
	2	2751.4	0.8	1.7	Laterite soil	
	3	1186.7	31.3	33.0	Ferruginous fine sand	KH
	4	3111.9	--	--	Ferruginous medium to coarse sand	
2	1	134.6	0.7	0.7	Topsoil	
	2	4297.8	5.9	6.6	Laterite soil	
	3	504.3	8.5	15.1	Ferruginous fine sand	KH
	4	3127.4	--	--	Ferruginous medium to coarse sand	
3	1	409.3	0.5	0.5	Topsoil	
	2	985.8	4.2	4.7	Laterite soil	
	3	1978.7	9.9	14.6	Sandy clay	AKH
	4	815.1	8.5	23.1	Ferruginous fine sand	
	5	3047.0	--	--	Ferruginous medium to coarse sand	
4	1	56.8	1.1	1.1	Topsoil	
	2	4261.2	1.2	2.2	Lateritic rock	
	3	737.9	7.9	10.1	Sandy clay	KHK
	4	3244.9	24.4	34.6	Ferruginous fine sand	
	5	625.9	--	--	Ferruginous medium to coarse sand	
5	1	55.8	1.1	1.1	Topsoil	
	2	4196.3	1.2	2.3	Laterite soil	
	3	2678.7	34.0	36.3	Ferruginous fine sand	KH
	4	603.0	--	--	Ferruginous medium to coarse sand	
6	1	81.5	0.4	0.4	Topsoil	
	2	225.6	2.0	2.5	Laterite soil	KH
	3	5477.8	12.8	15.2	Ferruginous fine sand	
	4	1406	--	--	Ferruginous medium to coarse sand	
7	1	195.5	0.6	0.6	Topsoil	
	2	1673.6	3.3	3.9	Laterite soil	KH
	3	1038.9	36.4	40.2	Ferruginous fine sand	
	4	3618.5	--	--	Ferruginous medium to coarse sand	
8	1	747.3	1.5	1.5	Topsoil	
	2	6472.2	2.9	4.4	Laterite soil	KH
	3	890.0	6.5	10.9	Ferruginous fine sand	
	4	2497.3	--	--	Ferruginous medium to coarse sand	
9	1	484.4	2.9	2.9	Topsoil	
	2	2000.0	18.3	21.2	Laterite soil	KH
	3	605.8	21.6	42.8	Ferruginous fine sand	
	4	4422.8	--	--	Ferruginous medium to coarse sand	
10	1	101.2	0.5	0.5	Topsoil	
	2	260.7	2.7	3.3	Laterite soil	KH
	3	983.7	5.7	9.0	Ferruginous fine sand	
	4	1324.9	--	--	Ferruginous medium to coarse sand	

11	1	128.3	1.1	1.1	Top soil	
	2	1081.1	14.3	15.4	Laterite soil	A
	3	2497.6	--	--	Ferruginous medium to coarse sand	
12	1	71.3	0.7	0.7	Top soil	
	2	406.3	3.4	4.0	Laterite soil	A
	3	1541.5	--	--	Ferruginous medium to coarse sand	

Geo-Electric Sections of the VES Points

Figure 4 shows a geo-electric section of the study area, the lithological differentiation ranges from top soil, dry sand, clayed sand, wet sand and sand stone. The majority of the top soil has thicknesses between 0.5 and 1.1 meters and resistivity values between 56 and 427 meters, the location with low overburden thickness of about 0.7m are regarded as areas with low protective capacity and low groundwater potential area, while those in location with highest overburden thickness are classify as location with high groundwater potential which was established in the research work of Zohdi *et al.*(2019) the VES2, VES3, and VES4 are located in low groundwater potential zones, which have little protective capacity and very little overburden thickness, they are unconsolidated layers which can allow contaminants inflow into groundwater zones. The VES 2 show a higher resistivity value of 4298Ωm which is a sand stone layer with a thickness of 5.9m, this indicates that the location might have little or no groundwater potential. The protective capacity is very low. Majority of the last layers compost of bedrock with higher resistivity values.

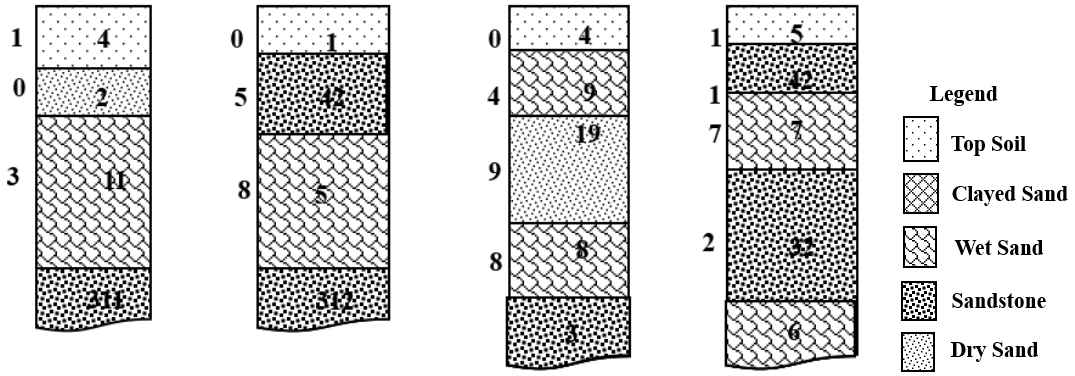

Figure 4: Geo-electric section of VES 1 to 4

Figure 5 shows a geo-electric section of the study area, the numerous types of lithology include clayed sand, wet sand, dry sand, top soil, and sand stone. Most of the top soil have resistivity values ranging from 56 Ωm to 747 Ωm with thickness ranging from 0.4 m to 1.5 m, VES 5, VES 6 and VES 7 locations are of low overburden thickness of 0.4 m and 0.6 m respectively, which are regarded as areas with low protective capacity and low groundwater potential area, while those in location with highest overburden thickness are classify as location with high groundwater potential which was established in the research work of Zohdi *et al.*(2019) VES 5 and VES 6 are unconsolidated layers that potentially let contaminants to enter groundwater zones; they are located in the low groundwater potential zones with very low overburden thickness and low protective capacity. Meanwhile, VES 7 and VES 8 show similar lithology of higher resistivity value of 1874 Ωm and 6472 Ωm which is an indication of a concealed bedrock before a fracture layer, in this location the groundwater is well protected especially the VES 8 because of high overburden thickness and still showed some level of fractures.

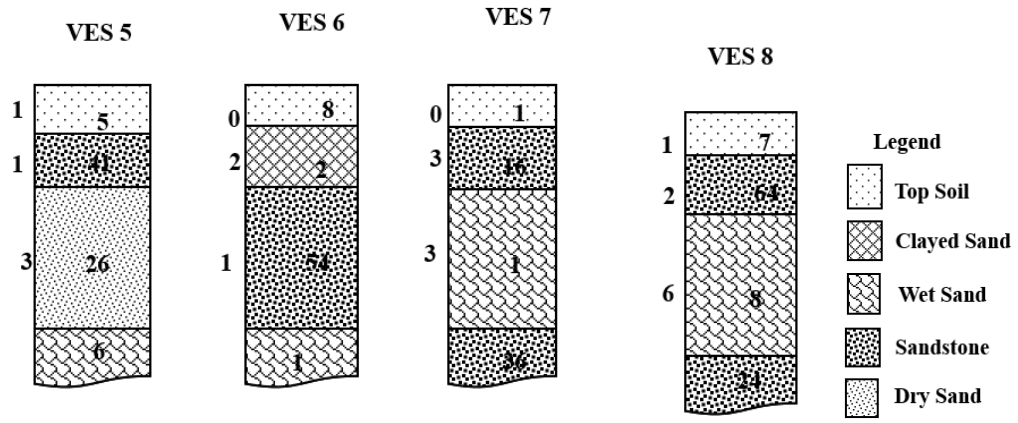

Figure 5: Geo-electric section of VES 5 to 8

Figure 6 shows a geo-electric section of the study area, the lithological differentiation ranges from top soil, dry sand, clayed sand, wet sand and sand stone. Most of the top soil have resistivity values ranging from 71 Ωm to 480 Ωm with thickness ranging from 0.5 m to 2.9 m, the location with low overburden thickness of about 0.7 m are regarded as areas with low capacity and low groundwater potential area, while those in location with highest overburden thickness are classify as location with high groundwater potential which was established in the research work of Zohdi *et al.*(2019), the VES 10 and VES 12 fall within the low groundwater potential zones with very low overburden thickness and low protective capacity, they are unconsolidated layers which can allow contaminants inflow into groundwater zones. The VES show a higher resistivity value of 2000 Ωm which is an indication of a concealed bedrock before a fracture layer, this location might have some groundwater. If the bedrock can be blast before getting to the fracture zone at VES 11, we have slightly different soil formation with a deeper aquifer of about 108 Ωm containing wet sand, but at this location the groundwater is well protected because of high overburden thickness. Majority of the last layers compost of bedrock with higher resistivity value especially at location VES 10 and VES 12, while location VES 9 and VES 11 still showed some level of deep fractures.

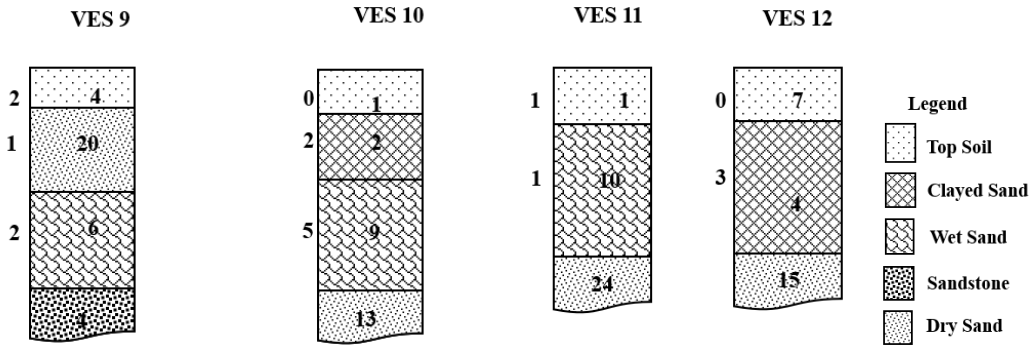

Figure 6: Geo-electric section of VES 9 to 12

Aquifer Protective Capacity (APC) Classification of the Study Area

The APC classification of the study area as revealed in (Table 2) is based on Oladapo and Akintorinwa, 2007, that the locations are of poor APC ratings due to some factors displayed in (Table 2) which makes the area vulnerable to contaminations.

Table 2: Aquifer Protective Capacity Rating of the Study Area

Location	RES 1 (Ω)	TH 1 (M)	RES 2 (Ω)	TH 2 (M)	RES 3 (Ω)	TH 3 (M)	RES 4 (Ω)	TH 4 (M)	RES 5 (Ω)	LC(APC)	APC Rating
Sagamu 1	427	1.0	2751	0.8	1187	31.3	3112			0.002633	POOR
Sagamu 2	135	0.7	4298	5.9	504	8.5	3127			0.006558	POOR
Sagamu 3	409	0.5	986	4.2	1979	9.9	815	8.5	3047	0.010485	POOR
Sagamu 4	57	1.1	4261	1.2	738	7.9	3245	24	626	0.01958	POOR
Sagamu 5	56	1.1	4196	1.2	2679	34	603			0.03262	POOR
Sagamu 6	82	0.4	226	2	5478	12.8	1407			0.016064	POOR
Sagamu 7	196	0.6	1674	3.3	1039	36.4	3619			0.005033	POOR
Sagamu 8	747	1.5	6472	2.9	890	6.5	2497			0.002456	POOR
Sagamu 9	484	2.9	2000	18.3	606	21.6	4423			0.015142	POOR
Sagamu 10	101	0.5	261	2.7	984	5.7	1325			0.015295	POOR
Sagamu 11	128	1.1	1081	14.3	2498					0.008594	POOR
Sagamu 12	71	0.7	406	3.4	1542					0.009859	POOR

NB: Aquiferous units are indicated with blue marker

Interpretation of 2D ERT Sections

Figures 7 (a–f) show the resistivity distribution and subsurface inverse model sections that were obtained via 2-D inversion. Every profile is 200 meters long, with the exception of profile 1, which is 180 meters long and served as the available area for conducting the study.

Figure 12a shows the pseudosection for profile 1 which covers a horizontal distance of 180 m along the ground surface. The topsoil has resistivity range of 330 to 676 Ωm from the beginning of the profile to 40 m distance from the ground surface to a depth of 13.00 m revealing a lithology of laterite soil transitioning into dry sand. From 40 m distance to 78 m along the profile is dry sand in the top soil having resistivity of 760 to 1250 Ωm from the ground level to a depth of 20.5 m. from 80 m distance to the end of the profile is loose dry sand of resistivity of 1300 to 1950 Ωm at the ground surface to ferruginous fine sand extending to a maximum depth beyond 24.9 m at the 120 m distance along the profile. This is followed by a ferruginous medium to coarse sand from distance of 50m to 120 m along the profile and from the depth of 17 m downward beyond 39.6 m depth covered by the inversion software. Figure 12b shows the pseudosection for profile 3 which covers a horizontal distance of 180 m along the ground surface. The topsoil has resistivity range of 330 to 663 Ωm from the beginning of the profile to 40 m distance from the ground surface to a depth of 12.80 m revealing a lithology of laterite soil transitioning into dry sand. From 40 m distance to 76 m along the profile is dry sand in the top soil having resistivity of 730 to 1200 Ωm from the ground level to a depth of 18.5 m. From 80 m distance to the end of the profile is loose dry sand of resistivity of 1400 to 1650 Ωm at the ground surface to ferruginous fine sand extending to a maximum depth beyond 31.9 m at the 120m distance along the profile. This is followed by a weathered/fractured layer of fresh basement from distance of 50 m to 120 m along the profile and from the depth of 17 m downward beyond 39.6 m depth covered by the inversion software. Figure 12c shows the pseudosection for profile 3 which covers a horizontal distance of 180 m along the ground surface. The topsoil has resistivity range of 330 to 637 Ωm from the beginning of the profile to 40 m distance from the ground surface to a depth of 7.50 m revealing a lithology of humid loamy soil transitioning into dry sand. From 40 m distance to 76 m along the profile is dry sand in the top soil having resistivity of 700 to 1300 Ωm from the ground level to a depth of 18.5 m. From 80 m distance to the end of the profile is loose dry sand of resistivity of 1350 to 2000 Ωm at the ground surface to conglomerate of sandstone extending to a maximum depth beyond 24.45 m at the 120 m distance along the profile. This is followed by a weathered/fractured layer of fresh basement of resistivity value of 2100 to 2300 Ωm from distance of 50 m to 120 m along the profile and from the depth of 24.9 m downward beyond 39.6 m depth covered by the inversion software. Figure 12d represent the pseudosection of profile 4. The topsoil has a depth up to 7.5 m covering a lateral distance of 180 m and resistivity range of 373 to 597 Ωm representing a mix of silt, sand and pebbles. This is followed by a layer of resistivity of 756 to 1211 Ωm from a depth of 7.5 m to 18 m spreading across the entire profile indicating ferruginous fine sand. The last identified layer in the profile is a layer of ferruginous medium to coarse sand of resistivity of 3208 to 4100 Ωm occuring at the depth of 18 m and below. The injected current terminated at this layer, for which the layer thickness cannot be determined. Figure 12e represent the pseudosection of profile 5. The topsoil has a depth up to 7.5 m covering a lateral distance of 180m and resistivity range of 343 to 597 Ωm representing a mix of silt, sand and pebbles. This is followed by a layer of resistivity of 650 to 1130 Ωm from a depth of 7.5 m to 18 m spreading across the entire profile indicating dry sand. From 80 m distance to the end of the profile is loose dry sand of resistivity of 1200 to 18500 Ωm at the ground

surface to ferruginous fine sand extending to a maximum depth beyond 39 m at the 120 m distance along the profile. This is followed by a ferruginous mediumto coarse sand of resistivity value of 1900 to 2309 Ωm from distance of 50 m to 120 m along the profile and from the depth of 17 m downward beyond 39.6 m depth covered by the inversion software. Figure 12f shows the pseudosection for profile 6 which covers a horizontal distance of 180 m along the ground surface. The topsoil has resistivity range of 720 to 1024 Ωm from the beginning of the profile to 40 m distance from the ground surface to a depth of 7.50 m revealing a lithology of laterite soil transitioning into dry sand. From 40 m distance to 76 m along the profile is dry sand in the top soil having resistivity of 1095 to 1450 Ωm from the ground level to a depth of 18.5 m. from 80 m distance to the end of the profile is loose dry sand of resistivity of 1500 to 2005 Ωm at the ground surface to ferruginous fine sand extending to a maximum depth beyond 18.5 m at the 120 m distance along the profile. This is followed by a weathered/fractured layer of fresh basement of resistivity value ranging from 2012 to 2315 Ωm from distance of 50 m to 120 m along the profile and from the depth of 24.9 m downward beyond 31.9 m depth covered by the inversion software.

(a)

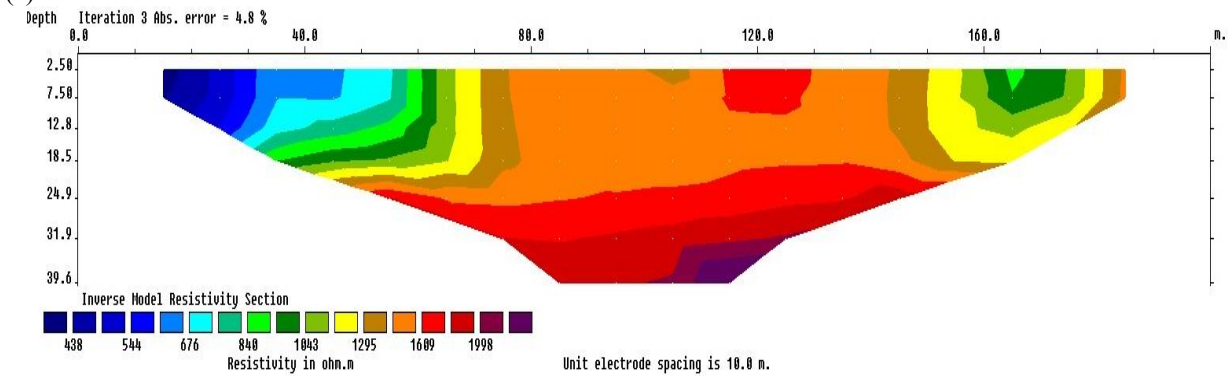

(b)

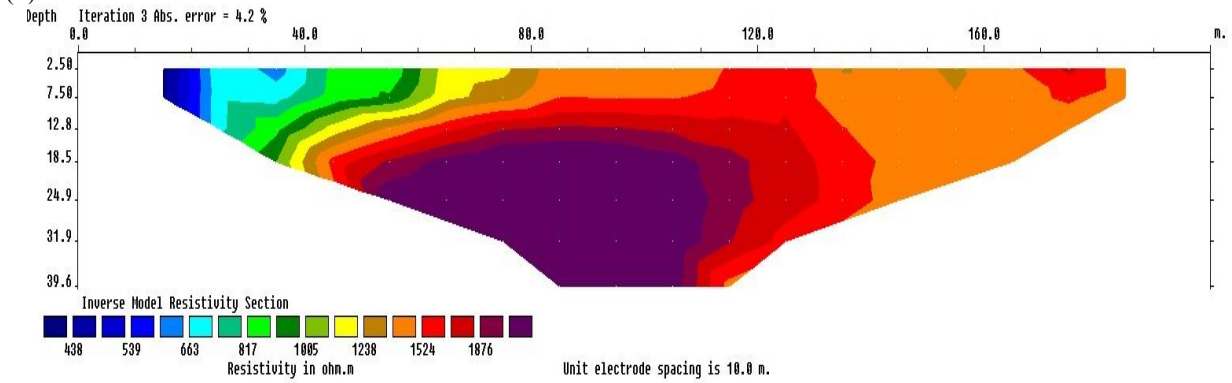

(c)

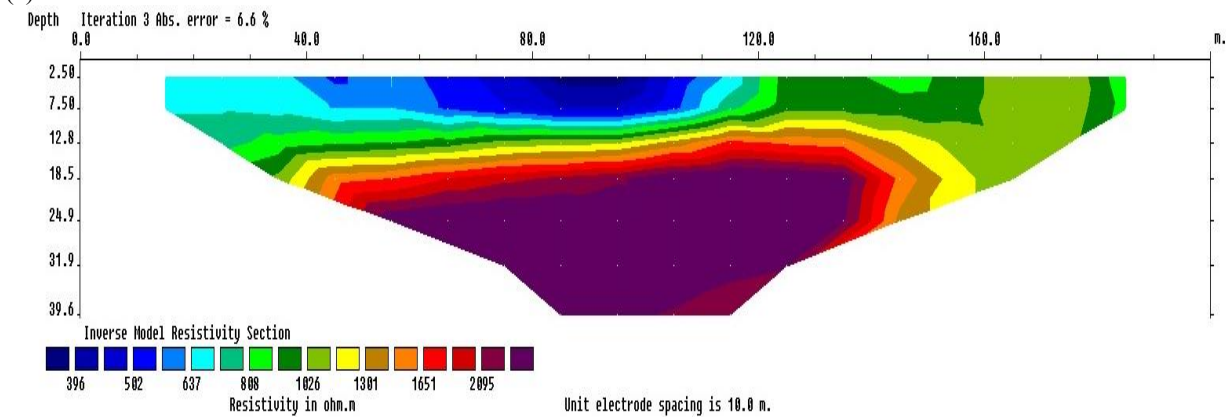

(d)

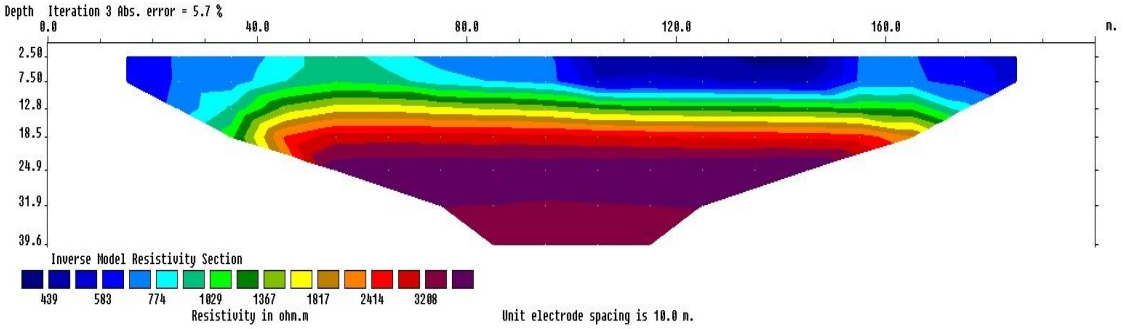

(e)

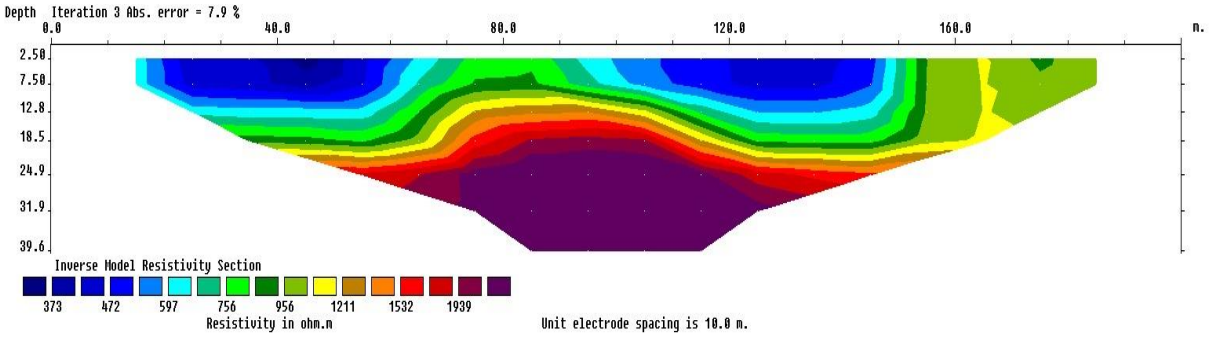

(f)

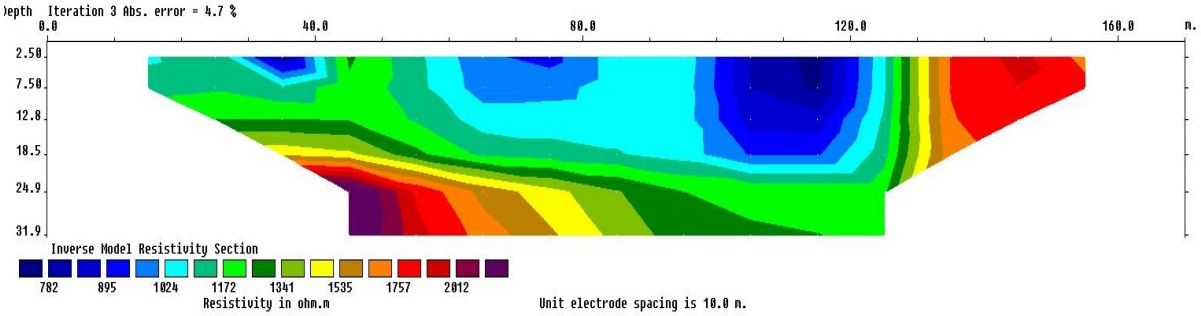

Figure 7 (a – f): 2D Resistivity Model Sections for profile 1 to 6

Natural Electric Field (NEF) Result

The NEF data processing was enhanced by the PQWT unique in-built computing functions software which by analog to digital sampling, a frequency curve graph with profile map is automatically generated (Kearey, 2012). Where lines of high resistivity converge or intersect to form an inverted basin (E1 and E2) (Figure 8a) indicate an extrusion rock formation (zone zero probability of getting groundwater/ water bearing zone). Profile L1 (Figure 8b) generally consists of a medium to hard rock formation. There is very low or zero chance of getting groundwater on the map (Figure 8b), especially at point 8 and 13 as it contained high resistivity, high Density, high potential value and hard rock formation / basement rock propagating from toward the earth surface but terminated at the depth of 22m and 25m respectively on map. Generally, it is not recommended to drill boreholes or wells in this location since the yield is anticipated to be extremely poor.

(a)

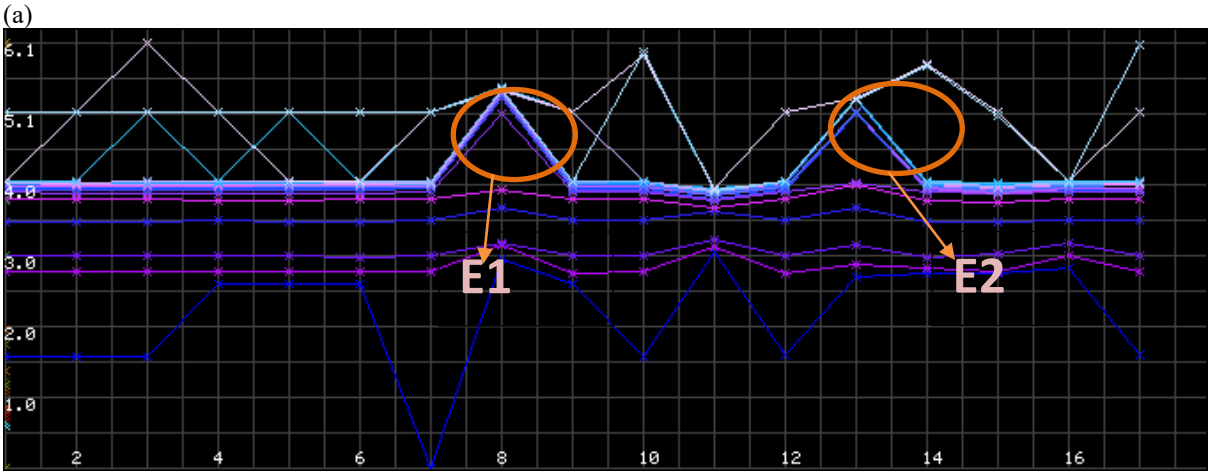

(b)

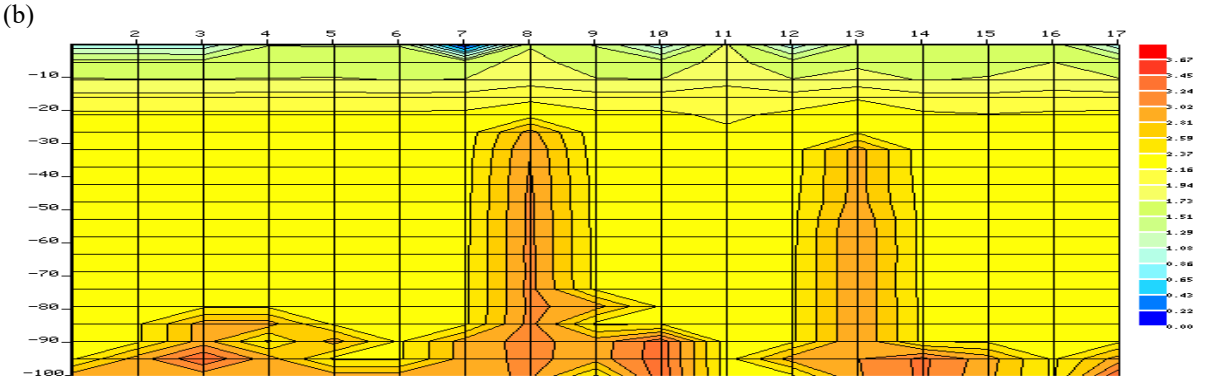

Figure 8 (a – b): A frequency curve graph with profile map and implication for profile L 1

A sudden change occurs in the homogeneity of the resistivity lines of the subsurface material rinsing from high to low S at point 11 (Figure 9a) which implies a sudden change from very hard to soft hard rock formation from point 1 – 6 at depth from 35 m – 100 m (Figure 9b). Profile L 2 has one major fracture bearing zones F (Figure 9a) on point 9 which is a zone with medium to high groundwater potential. Point 9 at a depth of 100 m is a good point for well recommendation with an overburden of 15 m. A fairly good - moderate yield should be expected.

(a)

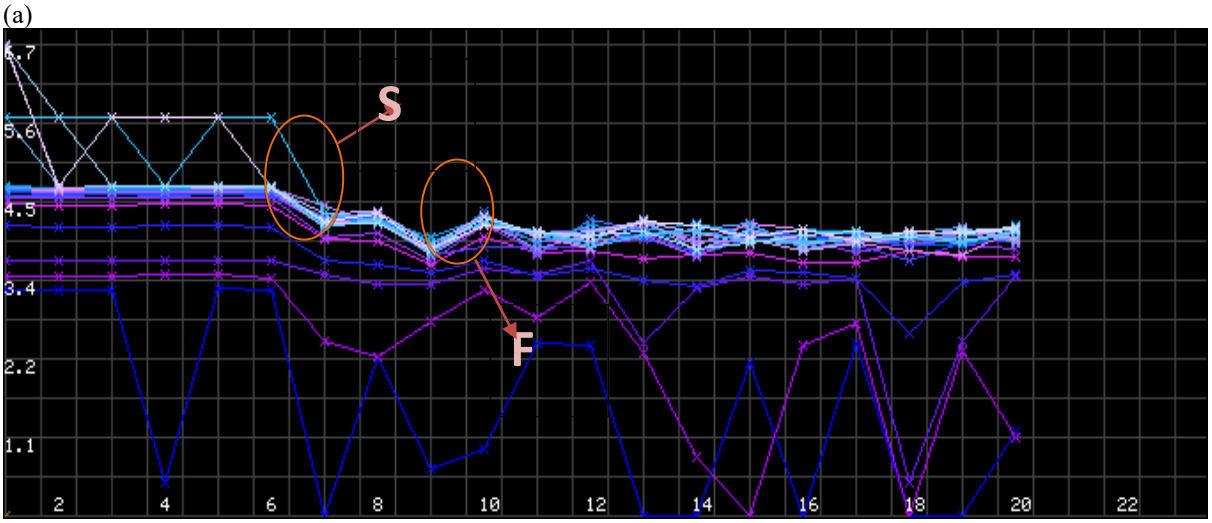

(b)

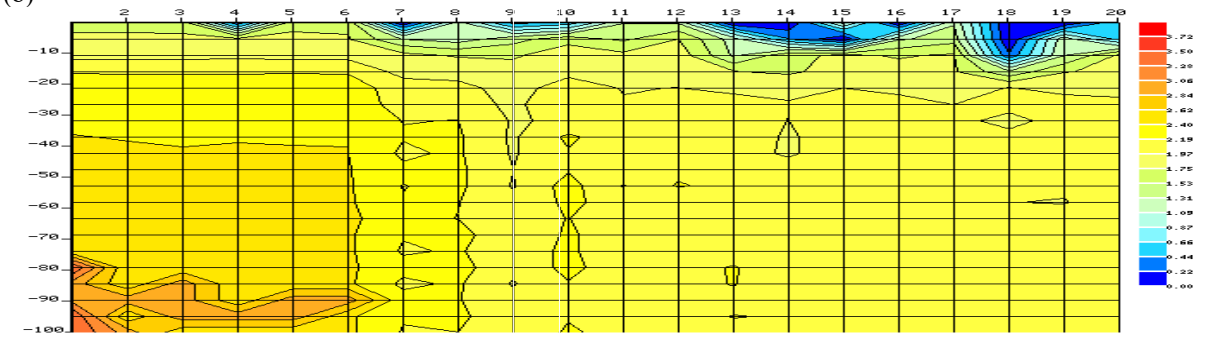

Figure 9 (a – b): A frequency curve graph with profile map and implication for profile L 2

The lines of different resistivity converge or intersect to form a basin at point 15(F) (Figure 10a) indicate a fractured/weathered zone (high probability of getting groundwater/ water bearing zone). A vertical crack of highly resistive, high density, high potential value and hard rock formation/material was observed at point 15, which is in between point 14 and 16 at depth of 30m (Figure 10b) thereby, allowing a formation of low resistive, low density, low potential value and soft rock formation /material in between high resistive material which make point 15 a high groundwater potential zone. Drilling well can be carried out at point 15 with an overburden of 25 m. A medium - high yield should be expected.

(a)

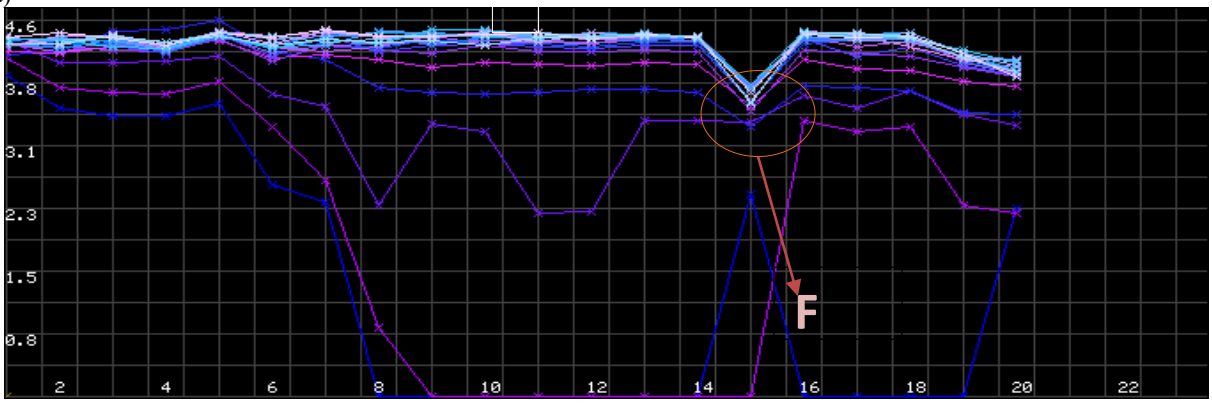

(b)

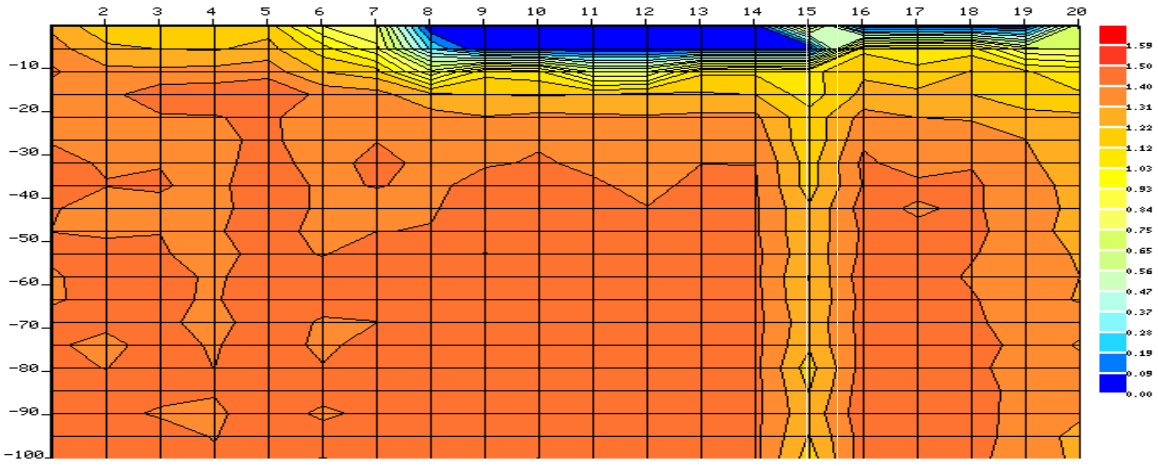

Figure 10 (a – b): A frequency curve graph with profile map and implication for profile L 3

There is a change occurs in the homogeneity of the resistivity lines of the subsurface material rinsing from low to high S at point 15 (Figure 11a) which implies a sudden change from soft to very hard rock formation from point 15 – 19 at depth from 35 m – 100 m (Figure 11b). Points 10, 12, 13 and 14 are good zones for groundwater potentials while point 14 has major fracture/ weathered materials which cut through from depth of 4 – 100m and therefore indicates high potential bearing zones F (Figure 11b) and this feature makes point 14 more prolific than other points on the map. Point 14 at a depth of 100 m is a good point for well recommendation with an overburden of 23 m. A moderate - high yield should be expected.

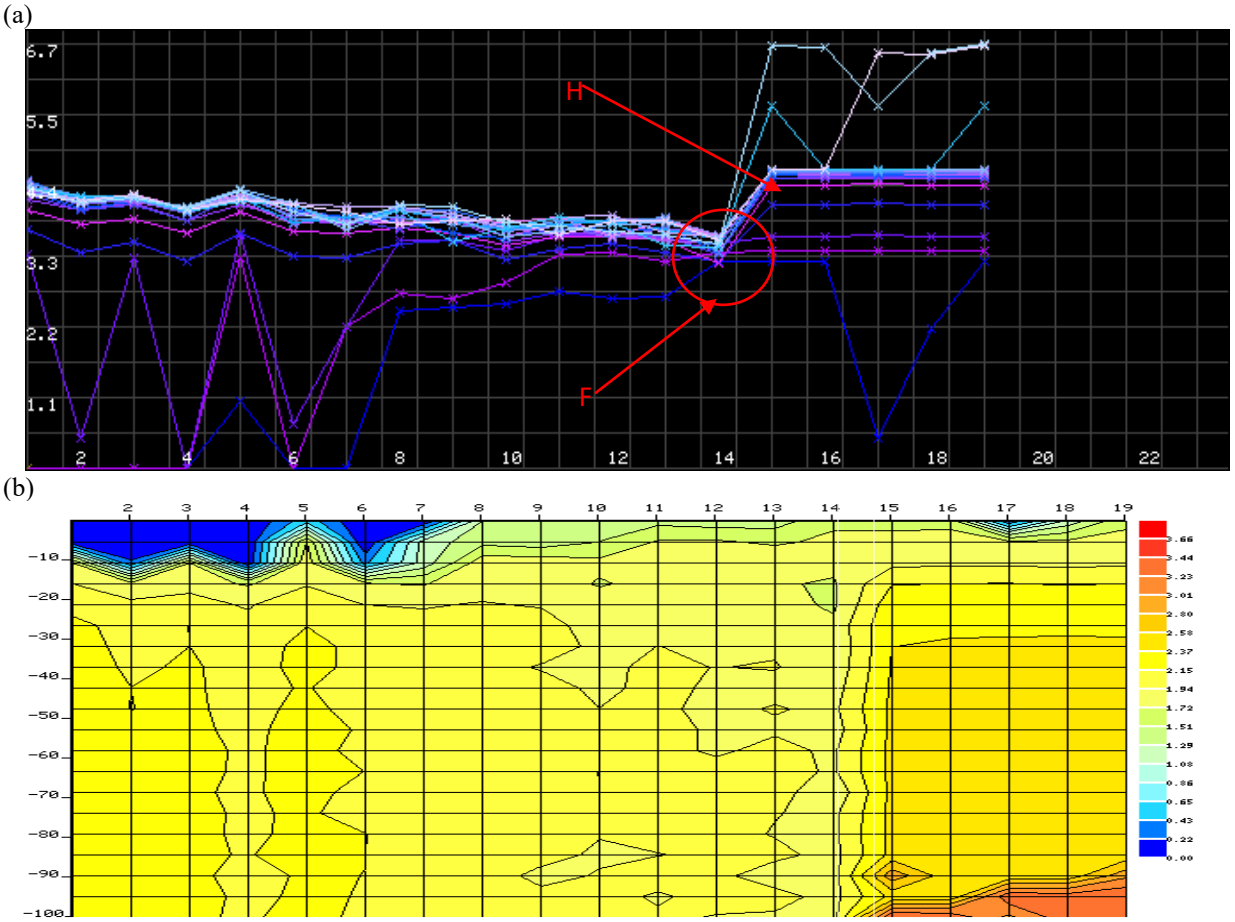

Figure 11 (a – b): A frequency curve graph with profile map and implication for profile L 4

The subsurface material formation is homogeneous (H) in profile L5 due to the series of straight / parallel resistivity lines (Figure 12a). Profile L5 generally consists of a soft to very hard rock formation. At depth 1-15 m consists of subsurface materials that are of low resistivity, low density, soft and low potential value while at depth of 15-80 m consists of medium resistivity, medium density and medium potential value subsurface materials. High resistivity, high density, high potential value, and hard rock formation basement rock are found at depths of 80–100 m (Figure 12b). It is not advised to drill wells because of the low yield (low groundwater potential) shown on this map.

(a)

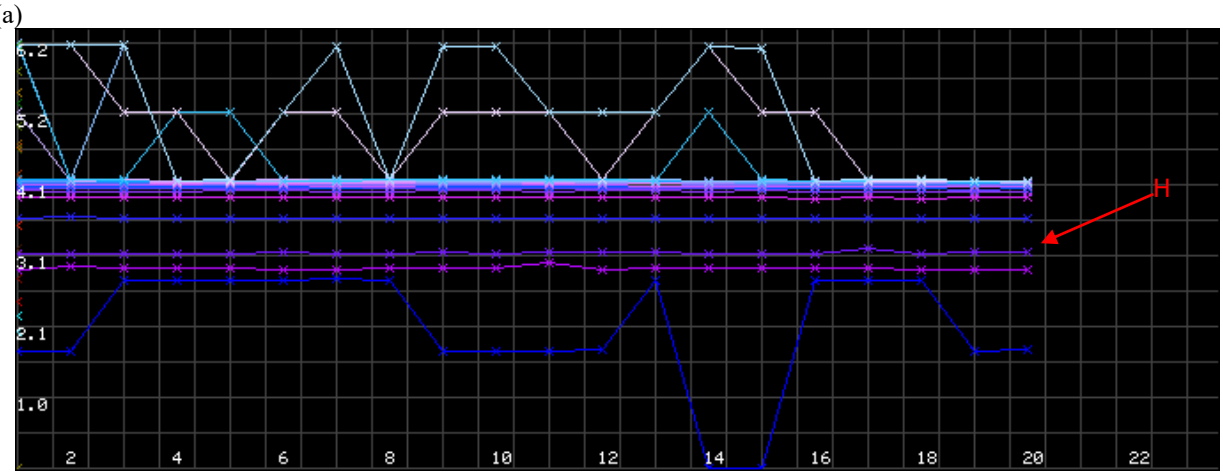

(b)

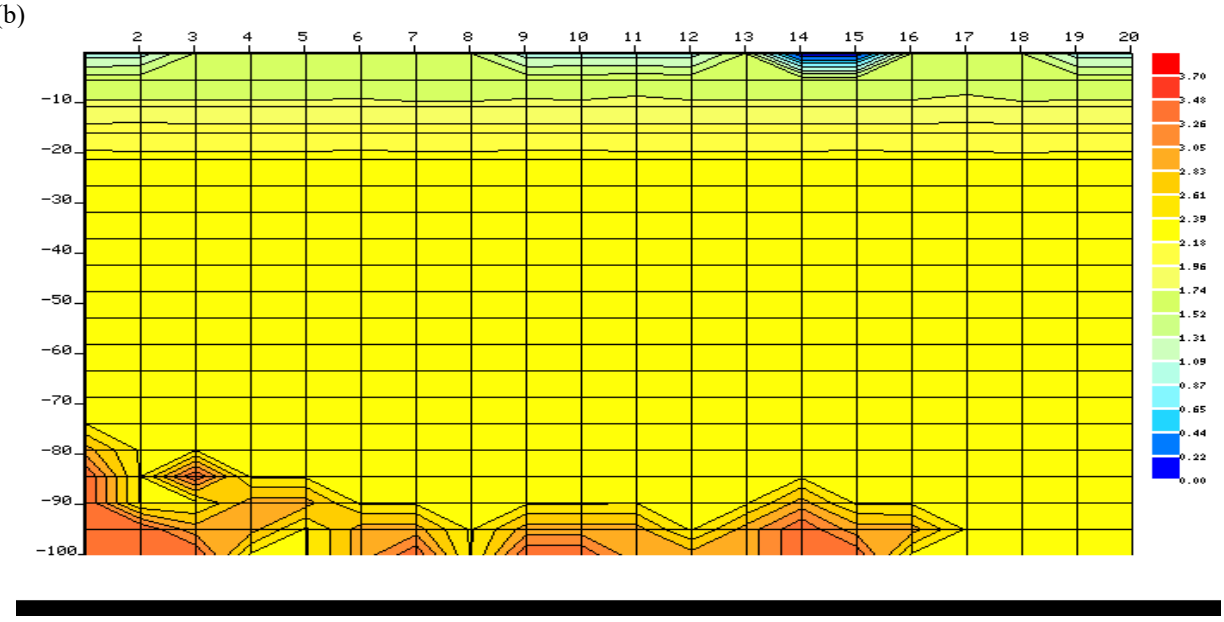

Figure 12 (a – b): A frequency curve graph with profile map and implication for profile L 5

The succession of parallel/straight resistivity lines in profile L6 indicates that the underlying material formation is homogenous (H) (Figure 13a). The rock formation in Profile L6 is typically soft to very hard. Low resistivity, low density, soft, and low potential subterranean materials are found at depths of 1 to 15 meters, whereas medium resistivity, medium density, and medium potential subsurface materials are found at depths of 15 to 35 meters. Hard rock formation/basement rock, high resistivity, high density, and high potential value are found at depths of 80–100 m (Figure 13b). This map indicates a low yield (zero to low groundwater potential); as a result, well drilling is not advised.

(a)

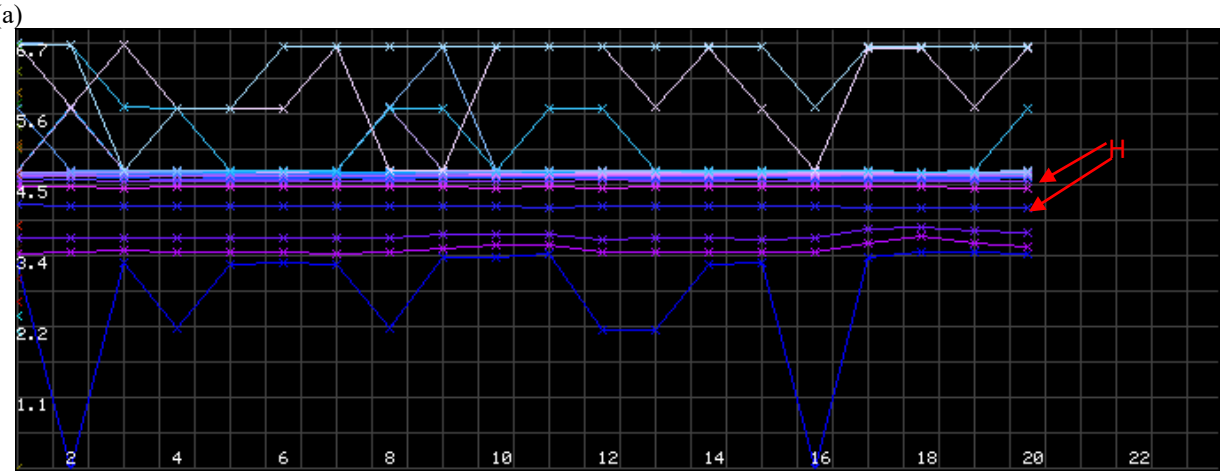

(b)

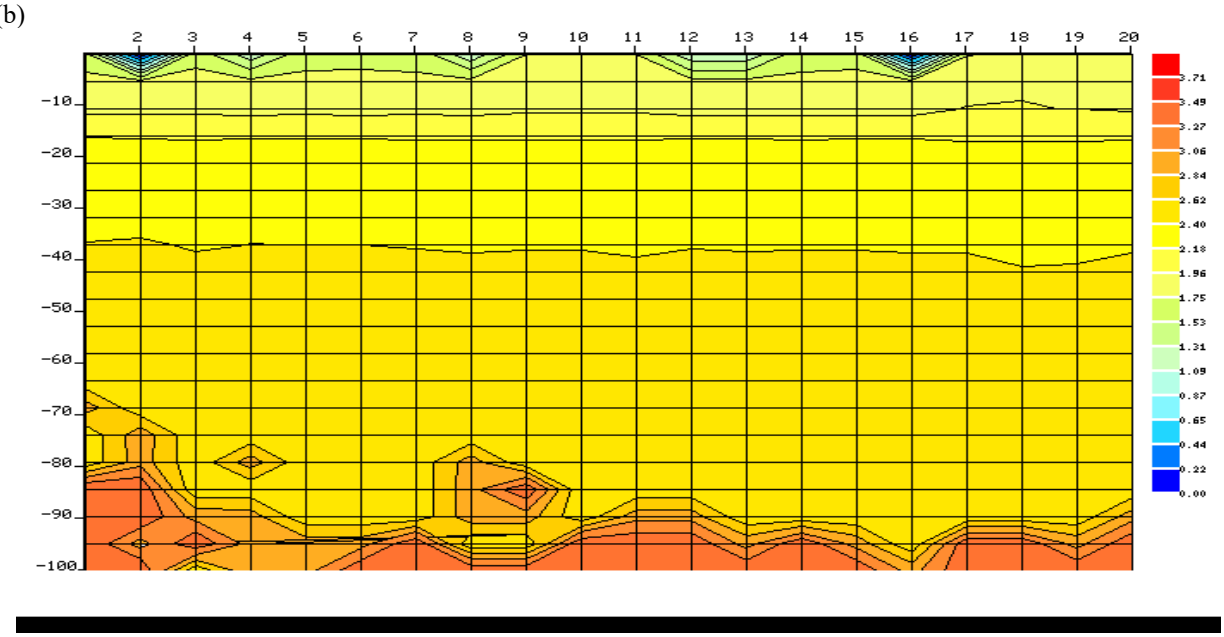

Figure 13 (a – b): A frequency curve graph with profile map and implication for profile L 6

Dar Zarrouk Parameters for the VES Data

Longitudinal unit conductance (S)

As indicated in Table 3, the longitudinal conductance values in this investigation were categorized into poor, weak, moderate, good, very good, and excellent protective capacity zones in accordance with Oladapo *et al*. (2004). The longitudinal conductance values are summarized in Table 4. All the VES station except VES station 4 falls under poor protective capacity zones with S value ranging from 0.01 to 0.06 while VES station 4 with S value of 0.13 falls under weak protective capacity zone. The study area is prone to infiltration (contaminations) due to low longitudinal conductance values (Poor – weak protective capacity value).

Table 3: Modified the Longitudinal conductance/protective Aquifer Capacitive rating (Oladapo *et al*. 2004)

Longitudinal Conductance	Protective Capacity Rating
>10	Excellent
5-10	Very good
0.7-4.9	Good
0.2-0.69	Moderate
0.1-0.19	Weak
<0.1	Poor

Table 4: Longitudinal Conductance and Protective Capacity Rating for the VES

VES No	Longitudinal Conductance (Ω^{-1})	Protective Capacity Rating
1	0.05	Poor
2	0.03	Poor
3	0.03	Poor
4	0.13	Weak
5	0.02	Poor
6	0.02	Poor
7	0.03	Poor
8	0.01	Poor
9	0.06	Poor
10	0.05	Poor
11	0.03	Poor
12	0.02	Poor

Groundwater Potential

Transverse resistance (T) and transitivity (A) are directly correlated; the aquifers or aquiferous units with the highest T values are probably those with the highest T values, and vice versa (Anudu et al., 2011 Kumar et al., 2001). Vertical electrical sounding stations such as VES 1, 2, 3, 7, 9 and 10 with computed transverse resistance greater than 20000 Ωm^2 but less than 50000 Ωm^2 are defined as areas of medium groundwater potentials while VES station 6 with transverse resistance value of 88193.90 (Ωm^2) is define as area with high groundwater potentials. VES stations 4, 5, 8 ,11and 12 are define as areas with low groundwater potential due to their low transverse resistance values as shown in table 10. The higher Anisotropy values (2.04, 2.35, 2.36, 2.56, 1.76, 2.38, and 2.20) observed at VES station 1, 2, 3, 6, 8, 9, and 10 respectively relates to how hard and compacted rocks are. (Keller and Frischknecht, 1966), which implies that the anisotropic nature of the aquifers is associated with low porosity and permeability (low potential groundwater zone) while VES stations 4, 5, 7, 11 and 12 with coefficient of anisotropy less than 1.5 (high porosity and permeability) are consider as high groundwater potential zones (Rao *et al*., 2003) Longitudinal resistivity value of the VES points (Table 5) of the study area shows the values ranging between (41.30 – 898.86) Ωm, while most of the study area is covered by values between (315.78 – 898.86) Ωm. VES station 6, 8 and 11 reveals very high longitudinal resistivity from (812.04 - 898.86) Ωm, while those at the remaining VES stations show values ranging between 41.30 – 486.24 Ωm. Less longitudinal resistivity than transverse resistivity was found in the current study, indicating the presence of various layers beneath the earth's surface (Flathe, 1955). The research area's transverse resistivity (ρt) reveals (Table 9) that high values between 1974.61 Ωm and 5879.59 Ωm are found in one section of the study area, while low values range from 63.77 Ωm to 971.39 Ωm inside another. The greatest value was noted at VES station 6. No layer significantly affects the transverse resistivity. The aquiferous character of the basement rocks can be inferred from the reflection coefficient and resistivity contrast at the fresh basement rock interface. Olayinka (1996) noted that a location with a lower reflection coefficient value has a larger water potential because it shows a fracture of the basement rock. Reflection coefficient and resistivity contrast values below 0.9 and 1 are used in this investigation (VES stations such as 6 and 11; Table 6, respectively, may be indicative of high-density water filled fracture (Anudu *et al*., 2011; Olayinka *et al*., 2000).

Table 5: Shows result of Dar Zarrouk (DZ) parameters estimated from the geo-electric layers

VES NO	Longitudinal Resistivity (Ω-m)	Overburden Thickness (m)	Transverse Resistance (Ωm^2)	Coefficient of Anisotropy	Reflection Coefficient	Resistivity Contrast	Presence of Weathered /fractured Basement	Transverse Resistivity
1	453.16	23.10	43769.90	2.04	0.99	273.08	_____	1894.80
2	438.43	12.10	29412.80	2.35	0.86	13.35	_____	2430.81
3	420.04	11.00	25731.90	2.36	0.87	14.76	_____	2339.26
4	41.30	5.40	328.24	1.21	0.95	43.00	Fractured	60.79
5	61.55	1.10	70.15	1.02	0.92	24.90	_____	63.77
6	898.86	15.00	88193.90	2.56	0.74	0.15	Fractured	5879.59
7	790.32	23.40	22730.60	1.11	0.67	5.13	_____	971.39
8	812.04	7.10	17876.10	1.76	0.62	4.30	_____	2517.76
9	349.34	19.70	38899.80	2.38	0.95	39.71	_____	1974.61

10	315.78	17.00	25983.00	2.20	0.72	6.26	_____	1528.41
11	848.38	24.10	11487.90	0.75	0.97	0.01	Fractured	476.68
12	486.24	11.90	9558.08	1.29	0.33	2.00	_____	803.20

Table 6 shows the summary of the groundwater potential estimated Dar Zarrouk (DZ) parameters estimated of the geo-electric layers.
After a careful review of the DZ parameters of the geo-electric layers of each VES station
(Table 5), the groundwater potential is classified into 3 categories (based on Table 6);
Low yield groundwater potential zones which consist of VES 2, 3, 8, 9, 10 and 12
Medium yield groundwater potential zone. VES 1 and 7 falls under this category
High yield groundwater potential zone in which VES 4, 6 and 11 are considered to be in the category.

Table 6: Groundwater Potential of Different VES Stations

VES No	Location	Groundwater Potential Remark
1	Lat 6.867412 Long 3.673843	Medium
2	Lat 6.866997 Long 3.674395	Low
3	Lat 6.867758 Long 3.673407	Low
4	Lat 6.865663 Long 3.674482	High
5	Lat 6.866463 Long 3.675002	Low
6	Lat 6.865973 Long 3.675428	High
7	Lat 6.867905 Long 3.674277	Medium
8	Lat 6.868038 Long 3.675168	Low
9	Lat 6.868152 Long 3.676035	Low
10	Lat 6.867557 Long 3.672505	Low
11	Lat 6.866365 Long 3.673817	High
12	Lat 6.866983 Long 3.673212	Low

CONCLUSION

The geophysical techniques identified five geoelectric layers: ferruginous medium to coarse sand, sandy clayey and ferruginous fine sand, topsoil, and laterite soil. In the laterite soil layer, the resistivity values varied between 55.5 and 747.3 Ωm, while the thickness ranged between 0.4 and 2.9 m. Between 225.6 and 8985.8 Ωm and the sandy clay layer's resistivity values ranged from 504.3 to 5477.8 Ωm, while its thickness ranged from 0.8 to 18.3 m; and finally, the layer of ferruginous medium to coarse sand had an infinite thickness. The range of the overburden thickness is 1.2 to 24.0 meters. The ferruginous fine sand layer of the VES stations constitutes the main aquifers' zone. However, the consequence of this research work indicated that 58.3% of all the VES points investigated had low to very low groundwater potential, 16.7% of the VES points constitute medium groundwater potential while the remaining 25.0% were fracture / high groundwater potential zones.

REFERENCES

Adabanija, M.A., Kolawole, L.L., Kolawole, A.O., and Osinowo, O.O. (2021) "Investigating aquifer structure in a low latitude crystalline basement complex of southwestern Nigeria using radial vertical electrical sounding, "Arabian *Journal of Geosciences,* 14 (4):1 – 4.

Agagu. O.K. (1985). A geological guide to bituminous sediments in Southwestern Nigeria. Unpublished Report, Department of Geology, University of Ibadan.

Agyemang, V.O. (2021). Hydrogeophysical characterization of aquifers in Upper Denkyira East and West Districts, Ghana. Applied Water Science,11:132. https//doi.org/10.1007/s13201-02101462-w.

Akoji, J.N. (2019). Evaluation of groundwater quality in some rural areas of the Federal Capital Territory, Abuja, Nigeria. Evaluation 7 unn.edu.ng.

Alabi, A.A., Popoola, O. I., Olurin, O.T., and Ogungbe, A.S. (2020). Used an integrated approach involving geophysical and physiochemical methods to assess the potential availability of groundwater and its quality at Akole, Abeokuta Southwestern Nigeria. *Journal of Environmental Earth Sciences* 79:364.

Alabi, A.A., Ganiyu, S.A., Idowu, O.A., Ogabi, A.F., and Popoola, O.I. (2021). Investigation of groundwater potential using integrated geophysical methods in Moloko-Asipa, Ogun State, Nigeria. Applied Water Science 11:70. (along Ife-Ede Road, South-Western Nigeria).

Anudu, G.K., Stephenson, R.A., and Macdonald, I.M. (2011). Using high-resolution aeromagnetic data to recognise and map intra-sedimentary volcanic rocks and geological structures across the Cretaceous middle Benue Trough, Nigeria. *Journal of African Earth Sciences* 99 (2):625 – 636.

Bayewu, O.O., Oloruntola, M.O., Mosuro, G.O., Laniyan, T.A., and Ariyo, S.O. (2017). Geophysical evaluation of groundwater potential in part of southwestern Basement Complex terrain of Nigeria using two geophysical methods, Very Low-Frequency Electromagnetic (VLF-EM) and Vertical Electrical Sounding (VES). *Appl Water Sci* 7:4615-4632. https://doi.org/10.1007/s13201-017-0623-4.

Desersa, T.T, Hassan, R., and Ringler, C. (2008). Measuring Ethiopian farmers' vulnerability to climate change across regional states. IFPRI Discussion Paper 806. Washington, D.C: IFPRI.

Falade, A.O., Amigun, J.O., and Kafisanwo, O.O. (2019). Application of electrical resistivity and very low frequency electromagnetic induction methods in groundwater investigation in ilara-mokin, Akure Southwestern Nigeria. Environ Earth Sci Res J 6(3):125–135.

Gaikwad, S., Pawar, N.J., Bedse, P., Wagh, K and Kadam, A. (2021) "Delineation of groundwater potential zones using vertical electrical sounding (VES) in a complex bedrock geological setting of the West Coast of India," *Modeling Earth Systems Environment*. 8: 2233-2247. https://doi.org/10.1007/s40808-021-01223-3.

Ganiyu, S.A., Oyadeyi A.T., Rabiu, J.A., Jegede, O.A. (2022). Hydrogeochemical categorization and quality assessment of shallow groundwater sources in typical urban slum and peri-urban areas of Ibadan, southwestern Nigeria. Environ Earth Sci 81:111. https://doi.org/10.1007/s12665-02210237-8.

Gobashy, M.M., Metwally, M., Abdeazeem, M., Soliman, K.S., and Abdelhalim, A. (2021). Geophysical Exploration of shallow groundwater aquifers in arid regions: A case study of Siwa Oasis, Egypt. Natural Resources Research 30 (5):3355 – 3384.

Ifeanyichukwu, K.A., Okeyeh, E., Agbasi, O.E., Moses, O.I., and Ben-Owope, O. (2021). An assessment of the groundwater potential of the farm with preliminary geophysical method and grain size analysis prior to the drilling of bore holes. HyroResearch. 5:85 – 98.

Joel, E.S., Olasehinde, P.I., Adagunodo, Omeje, M., Ifeanyi Oha, Akinyemi, M.I., and Olawole, O.C. (2020). Geo-investigation on groundwater control in some part of Ogun State using data from Shuttle Radar Topography Mission and vertical electrical sounding. Hellyon 6:1.

Kahal, A., Hussain, A., Abdelbaset, S.E., Qaysi, S., Fahad, A., and Faisal, K.Z. (2021). Evaluation of heavy metal contamination and groundwater quality along the Red Sea coast, southern Saudi Arabia. Maine pollution bulletin 163: 111975.

Keller, G.V. and Frischknecht, F.C., (1966). Electrical Methods in Geophysical Prospecting. Pergamon Press, Oxford.

kumar, S., Wesnousky, S.G., and Seitz, G.G. (2001). Earthquake Recurrence and Rupture Dynamics of Himalayan Frontal Thrust, India. *Science.* 294(5550). 2328-2331 https://doi.org/10.1126/science.1066195

Loke, M.H., and Barker, R.D. (1996). Practical techniques for 3D Resistivity surveys and data inversion. Geophysical prospecting, 44:499-524.

Mosuro, G., Bayewu, O., and Oloruntola, M. (2011). Geophysical investigation for groundwater exploration in Kobape via Abeokuta SW, Nigeria, https://doi.org/10.13140/2.1:4183.1686.

Muchingami, A., Mkali, L., Vinqi, T. (2021). "Integration of hydro-geophysical and geological

investigations in enhancing groundwater potential assessment in Houtriver gneiss crystalline basement formation of South Africa," Physics and Chemistry of the Earth, Parts A/B/C. 123. pp 103009.

Oladele, S., and Odubote, O. (2017). Aquifer mapping and characterization in the complex transition zone of Ijebu Ode, Southwestern Nigeria. Forum Geografic XVI (1): 49-58. https://doi.org/10.5775/fg.112.i.

Oladapo, M.I., and Akintorinwa, O.J. (2007). Hydrogeophysical study of Ogbese South Western Nigeria. *Global Journal of Pure and Applied Sciences* 13 (1):55 – 61.

Oladapo, O.T., Soyunsa, J.O., and Sule-Odu, A.O. 2004. The rise in caesarean birth rate in Sagamu: reflection of changes in obstetric practice. *Journal of Obsterics and Gyneacology* 24 (4):377 – 381.

Oladunjoye, M.A., Korede I.A., Adefehinti, A. (2019): Geoelectrical exploration for Ibadan, groundwater in crystalline basement rocks of Gbongudu community, southwestern Nigeria. Global Journal of Geological Sciences, 17:25-43.

Olatinsu, O. B., and Salawudeen, S.Y. (2021). "Integrated geophysical investigation of groundwater potential and bedrock structure in Precambrian basement rocks of Ife, southwest Nigeria," Groundwater for Sustainable Development. 14:100-616.

Osinowo, O.O., and Olayinka, A.I. (2012). Very low frequency electromagnetic (VLF-EM) and electrical resistivity (ER) investigation for groundwater potential evaluation in a complex geological terrain around the Ijebu-Ode transition zone, southwestern Nigeria. J Geophy Eng 9(4): pp 374-396. https://doi.org/10.1088/1742-2132/9/4/374

Oyeyemi, K., Aizebeokhai, A.P., and Oladunjoye, M.A. (2015). Department of Geology, University of Ibadan, Nigeria. *International Journal of Applied environmental Sciences.* 10(4):1275 – 1288.

Perrone, D., Jasechko, S. (2017): Dry groundwater wells in the western United States. Environ Res Lett, 12:104002. https://doi.org/10.1088/1748.9326/aa8acO.

Rao, S.M., Nestor, D.B., Turnshek, D.A., Lane, W.m., Monier, E.M., and Bergeron, J. (2003). Low-Redshift Damped Lyα Galaxies toward the Quasars B2 0827+243, PKS 0952+179, PKS 1127–145, and PKS 1629+120* © 2003. The American Astronomical Society. All rights reserved. Printed in U.S.A. *The Astrophysical Journal.* 595(1):94-107 https://iopscience.iop.org/article/10.1086/377331/meta#fn-article-title-en-1

Salami, S.A., and Ogbamikhumi, A. (2017). Used vertical electrical sounding (VES) method to study geo-electrical investigation for groundwater potential of Ihievbe Ogben, Edo North, Nigeria. *Journal of Applied Sciences and Environmental Management*. 21(7):1291-1296.

Sasaki, Y. 1994. 3D Resistivity inversion using the finite element method Geophysics, 59: 1839-1848.

Soomro A., Qureshi A.L., Jamali, M.A., Ashraf, A. (2019): Groundwater investigation through vertical electrical sounding at will area from. Nooriabad onward Karachi Acta Geophysica. https://doi.org/10.1007/s11600-019-00247-9

Tajudeen, F.P., Jaafar, N.I., and Sulaiman, A. (2019). Journal of open innovation. Technology, Market, and Complexity 5 (4):97-107.

Telford, W. M., Geldart, L. P., and Sherif, R. E. (1990). Resistivity method in Applied Geophysics, 2nd Edition Cambridge University Press, Cambridge, UK, Pp 353-358.

Tijani, M. 2019. Impacts of land-use changes and urbanization on coastal groundwater resources of Lagos Southwest Nigeria: Integrated hydrogeochemical and GIS-based assessments. Groundwater Management and Governance Coping with Uncertainty, Pp 269.

Wu, G., Chen, G., Wang, D., Cheng, O., Zhang, Z. and Yang, J. (2020). Identifying mineral prospectivity using seismic and potential field data in the Hongniangyu district, Inner Mongolia, China. Ore Geology Reviews 119:103317.

Zohdi, N., Tareq, s. and Yang, C. (2019). Investigation on mechanical anisotropy of high impact polystyrene fabricated via fused deposition modelling. In Proceedings of International Conference on Mechanical and Manufacturing Engineering research and Practice, Sydny, Ausralia, 26:24-28.